

**AIR DATA AND SURFACE PRESSURE MEASUREMENT
FOR HYPERSONIC VEHICLES**

by

BRYAN H. KANG

S.B., University of Southern California
(1987)

SUBMITTED IN PARTIAL FULFILLMENT
OF THE REQUIREMENTS FOR THE
DEGREE OF

MASTER OF SCIENCE IN
AERONAUTICS AND ASTRONAUTICS

at the

MASSACHUSETTS INSTITUTE OF TECHNOLOGY
May 1989

© Massachusetts Institute of Technology 1989

Signature of Author _____
Department of Aeronautics and Astronautics
May 12, 1989

Certified by _____
Associate Professor R. John Hansman
Thesis Supervisor, Department of
Aeronautics and Astronautics

Accepted by _____
Professor Harold Y. Wachman
Chairman, Department Graduate Committee

MASSACHUSETTS INSTITUTE
OF TECHNOLOGY

JUN 07 1989

LIBRARIES
Aero



AIR DATA AND SURFACE PRESSURE MEASUREMENT FOR HYPERSONIC VEHICLES

by

BRYAN H. KANG

Submitted to the Department of Aeronautics and Astronautics
on May 12, 1989 in partial fulfillment of the the
requirements for the degree of Master of Science
in Aeronautics and Astronautics

ABSTRACT

The air data and propulsion state measurement requirements for advanced air breathing hypersonic vehicles were estimated based on anticipated trajectories and vehicle configurations. Stringent requirements result from the harsh thermal environment in which the sensors must operate and interaction between the flight control and propulsion control systems. Flow direction measurement is critical for high speed air-breathing engines such as the scramjet. Based on prior hypersonic air data systems on the X-15, SR-71, and the Space Shuttle, surface pressure based measurement systems such as the Shuttle Entry Air Data System (SEADS) appears to be the most promising candidates for advanced hypersonic vehicles. A SEADS-like forebody pressure distribution measurement for air data system combined with an inlet surface pressure array for active inlet control is considered to be the most viable technology. Due to stringent requirements on the air data and inlet control parameters, as well as the need to locate the surface pressure sensors in regions of extreme thermal load, rigorous pressure transducer requirements (0.1% accuracy at 3000°F orifice temperature) are considered necessary. Existing technology high precision pressure transducers were found to require active or passive cooling in a hypersonic air data system.

Thesis Supervisor: R. John Hansman
Associate Professor
Dept. of Aeronautics & Astronautics

ACKNOWLEDGMENTS

The author wishes to thank Prof. R.J. Hansman for valuable advice. Also, Prof. Martinez Sanchez, Lewis. M., P. Gibson from NASA Langley provided valuable information for this work. Finally the author wishes to thank his parent and peers at room 442 for their support. This work was supported by the Charles Stark Draper Laboratory.

TABLE OF CONTENTS

	ABSTRACT	1
	ACKNOWLEDGEMENTS	2
	TABLE OF CONTENTS	3
1.0	INTRODUCTION	6
1.1	Instrumentation Requirements	7
1.2	Overview	10
2.0	HISTORY OF HYPERSONIC PRESSURE MEASUREMENT	11
2.1	X-15 Air Data System	11
2.1.1	Sensor Problems Encountered During X-15 Operation	16
2.2	Shuttle Air Data System	16
2.3	SR-71	22
2.3.1	SR-71 Air Data System	22
2.3.2	SR-71 Propulsion Control System	24
3.0	PROJECTED SENSOR ENVIRONMENT	32
3.1	Vehicle Description	32
3.2	Potential Configurations	34
3.3	Flight Envelope	36
3.4	Sensor Environment	38
4.0	THE INSTRUMENTATION REQUIREMENTS IMPOSED BY THE FLIGHT AND PROPULSION CONTROL SYSTEM	42
4.1	Overview	42
4.2	Flight Control System	42

4.3	Propulsion System	43
4.3.1	Sensitivity of Scramjet Combustion to Thermodynamic Flow Conditions	44
4.3.2	Sensitivity of Scramjet Combustion to Vehicle Attitude and Trajectory	46
4.4	Propulsion Control System	49
5.0	PRELIMINARY AIR DATA MEASUREMENT SPECIFICATIONS	55
5.1	Angle of Attack	55
5.2	Side Slip Angle	58
5.3	Mach number	61
5.4	Dynamic Pressure	62
5.5	Static Pressure and Altitude	65
5.6	Inlet Pressure	65
5.7	Inlet Temperature	66
5.8	Shock Location	66
6.0	AIR DATA SENSING TECHNIQUES	68
6.1	Forebody Surface Pressure Measurement	70
6.1.1	Flow Modeling	72
6.1.2	Numerical Techniques	72
6.2	Propulsion State Sensing Techniques	73
7.0	PRESSURE MEASUREMENT TECHNIQUES	75
7.1	Pressure Sensing Orifice Considerations	75
7.1.1	Sources of Error	77
8.0	SENSOR SYSTEM THERMAL CONSIDERATIONS	83
8.1	Sensor Installation and Design Requirements	88
9.0	PRESSURE TRANSDUCER EVALUATION	90
9.1	Performance Requirements	90
9.2	Applicability of Current Technology Sensors	92

8.0 CONCLUSION

95

REFERENCES

96

1.0 INTRODUCTION

In this thesis, surface pressure measurement concepts and requirements for hypersonic vehicle instrumentation system are discussed based on functional requirements of the vehicle flight and propulsion control systems.

In the 1950's and 1960's, extensive hypersonic research was pursued to solve problems associated with ballistic reentry vehicles and high speed aircraft. The high supersonic and hypersonic flight regime was explored with research vehicles such as the X-15. Also several configurations of ramjet mounted winged missiles were tested to study the feasibility of the airbreathing engines.¹¹ These vehicles were limited to high supersonic speed ($M < 3.5$) because of the inherent limitation of ramjet combustion and the limitations of high temperature materials. Hypersonic flight vehicle research was then discontinued because the technology of the 60's could not provide efficient, operational propulsion systems for hypersonic vehicles, and the practical application for such high speed vehicles was not clear since the reliability of rocket systems was preferred over the potential efficiency of airbreathing hypersonic flight.

Hypersonic flight vehicle research was partially revived to study issues associated with the Space Shuttle reentry. However airbreathing propulsion was not a thrust of this effort.

In recent years, enthusiasm for hypersonic flight research has been revived by the promise of a fully reusable, horizontal take off, single stage to orbit flight vehicle with airbreathing engines. This vehicle (National Aero-Space Plane NASP) would potentially be very efficient.⁸ Full reusability and single stage to orbit capability provides saving in spacecraft construction costs and horizontal takeoff capability eliminates complicated

launch facilities. The airbreathing propulsion system provide the most significant advantage of this vehicle configuration. Using atmospheric oxygen significantly reduces oxidizer weights when compared to the rocket propulsion system with similar payload capability.

The design of this vehicle is, however, a difficult task. The technical requirements are a challenge to every aspect of current technology. Advances in high speed aerothermodynamics, high temperature material science, supersonic combustion propulsion system, and high temperature instrumentation techniques are necessary for the successful development of an airbreathing hypersonic vehicle.

1.1 INSTRUMENTATION REQUIREMENTS

Airbreathing hypersonic vehicle configurations pose stringent requirements on the instrumentation system for both flight and propulsion control systems. The instrumentation system functions as the nervous system to connect the propulsion and flight control system, as well as sending information to controllers, safety devices, and crew displays. In flight control system, air data parameters such as angle of attack, side slip angle, flight Mach number, and altitude are needed to stabilize the vehicle and follow desired trajectory. The flow direction parameters such as angle of attack and side slip would be used to supplement the Inertial Navigation System (INS) and flight control system. Perturbation in the vehicle attitude would result in tremendous error rate at high Mach numbers and deviation from the desired trajectory. Also flight Mach number and altitude are needed by the guidance system to remain within the airbreathing (Mach number , altitude) corridor. The measurement of these air data parameters is difficult due to high thermal loads which result from high Mach number flight.

Past experience with the supersonic turbojet and the ramjet engines suggest that active control of the airbreathing engines is essential for the efficient engine operation and the vehicle safety at high speed. Hypersonic airbreathing engines such as ramjets or scramjets pose stringent requirements on the observability of inlet flow quality. Diffuser pulsing and upstream flow instabilities are difficult to control in high speed combustion and often cause the engine to unstart. Unstart of an airbreathing engine occurs when pressure builds inside the combustor and results in flame out. A strong shock wave formed on front of the unstarted engine causes tremendous drag. For example, after several SR-71 reconnaissance aircraft were lost due to engine unstart, control modifications were implemented to cut off the second engine in the event of an engine unstart. In the case of a single stage airbreathing hypersonic vehicle, unstart would result in formation of strong shock in front of the airbreathing engine, and the large drag on the engine would likely cause structural failure. In addition, excessive pitching moment caused by the high drag may result in uncontrollable pitch instability and loss of the vehicle. Consequently, fault tolerant control of the air-breathing engine is critical.

In order to control the air-breathing engines, propulsion parameters such as inlet shock geometry, inlet pressure and temperature field, and combustor flow Mach numbers are needed. The propulsion control system would require high bandwidth sensor system, based on the study of the SR-71 pressure sensor bandwidth requirement for the normal shock location detection.⁶ The propulsion state measurement is difficult due to the extremely hostile, high temperature sensor environment.

Measurement of external air data parameters are needed for the propulsion system as well as the flight control system. Changes in angle of attack and side slip will cause drastic changes in inlet flow field. Slight perturbations in shock geometry, velocity and

pressure distribution inside the inlet from nominal design conditions can significantly reduce the combustion efficiency. The motion of the vehicle perturbs the flow field near the inlet and directly influences the combustion efficiency and combustion stability. Consequently, the measurement of air data parameters, including the air breathing engine inlet parameters, are essential to the propulsion control system. Therefore, the propulsion and flight control system may require simultaneous control.

The air data measurement requirements for hypersonic vehicles will provide unique difficulties due to the rigorous flight envelope. Due to the extreme heating rates, conventional intrusive probe instrumentation techniques are not applicable at hypersonic velocities because the intrusive probe structure would heat up and burn or melt. However, in principle, most of the air data parameters can be extracted from surface pressure measurements. Also, the propulsion state can be extracted from inlet surface pressure measurements. Surface pressure measurement techniques are nonintrusive as compared with protruding probe techniques. Surface pressure measurement technique is also thought to be more reliable than proposed optical techniques.

Surface pressure measurement technique has an inherent limitation which is a trade off between the pressure transducer operation temperature and the sensor system bandwidth. If the sensor system bandwidth requirement is high, then the pressure transducer should be placed close to the high temperature surface. The bandwidth and precision requirements on the sensor system will determine the pressure transducer thermal and accuracy requirements.

1.2 OVERVIEW

Prior experience in hypersonic air data and propulsion sensing is reviewed for the X-15, SR-71, and Shuttle Orbiter. Potential hypersonic flight envelopes, environmental conditions and vehicle configurations are presented to define the context of the measurement systems. The functional requirements for both flight control and propulsion control systems are defined. These functional requirements are used to derive the air data measurement specifications. The influence of air data parameters on both the flight control and propulsion control system is described. A preliminary set of specifications for required air data and propulsion parameters is developed. General air data measurement techniques are discussed. Measurement techniques which provide the required parameters through surface pressure measurements are described and the implications for pressure sensor performance are discussed. Finally the applicability of current pressure sensor technology is evaluated and factors such as active sensor cooling are considered.

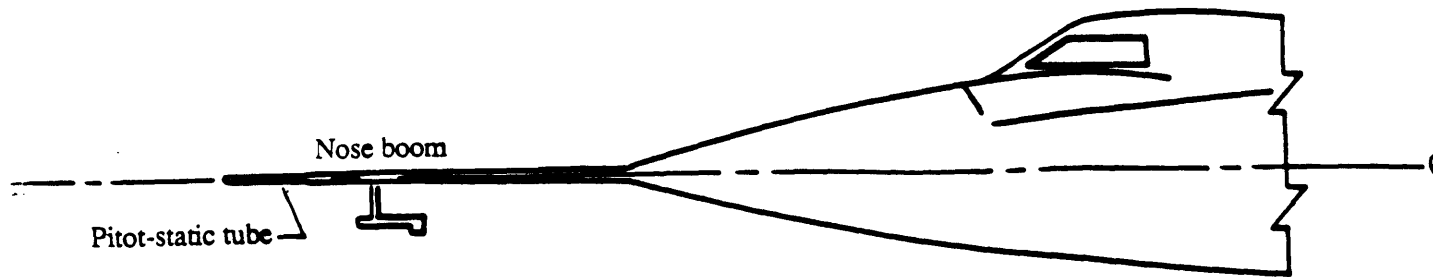
2.0 HISTORY OF HYPERSONIC PRESSURE MEASUREMENT

In the process of analyzing the air data sensing requirements for single stage air breathing hypersonic vehicle such as NASP, air data system of prior supersonic and hypersonic vehicles were reviewed. The SR-71, the X-15, and the Space Shuttle Orbiter have some analogous features to the single stage to orbit airbreathing hypersonic vehicle even though their primary mission and flight envelopes are different. The axisymmetric inlet sensors of the SR-71, the ball nose air data sensor of X-15, and the Shuttle from the Air Data System (ADS) are considered as technical precursors to the air data and propulsion instrumentation systems for future hypersonic vehicles.

2.1 X-15

The X-15 rocket propelled hypersonic research aircraft had typical missions of powered boost from 40Kft to about 200Kft with a ballistic coast to a maximum height of 350Kft. Reentry was accomplished by high angle of attack flight to dissipate energy while keeping the skin temperature within safe limits(1200°F). The hypersonic flight segment typically lasted 10 to 15 minutes.

For flight Mach numbers less than 3, the X-15 used a conventional pitot static nose boom with angle of attack and angle of side slip flow vanes as shown in Fig. 2.1.1. The X-15 experienced air data sensing problems at high Mach numbers ($M > 3$) due to high thermal load to the conventional vane-boom sensor. Also at high Mach numbers and at low dynamic pressures, the operational limits of the nose boom sensor are governed by the increase in vane position error due to a decrease in accuracy of the nose boom air flow direction measurements. The thermal constraints to the air data system was solved by "Ball Nose" air data sensor (Fig. 2.1.2). The sphere was housed in the end of the conic nose. It



Enlarged section of pitot-static tube end

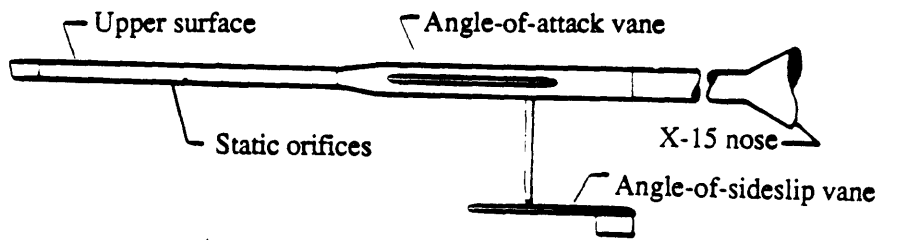


Fig 2.1.1 Schematic drawing of the X-15 nose-boom pitot-static tube with flow-direction vanes

taken from ref. 4

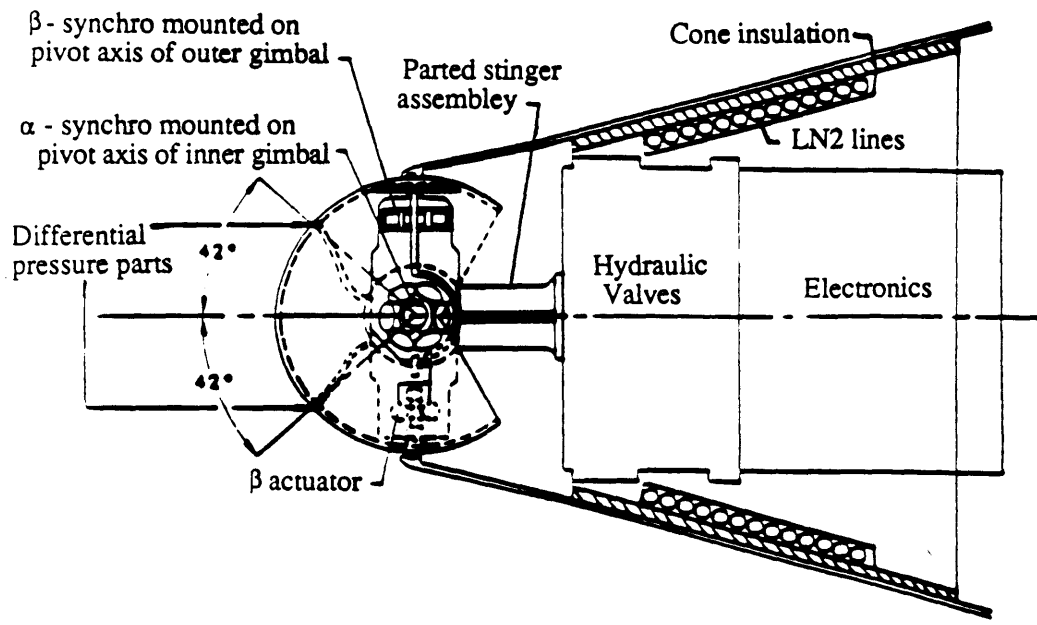
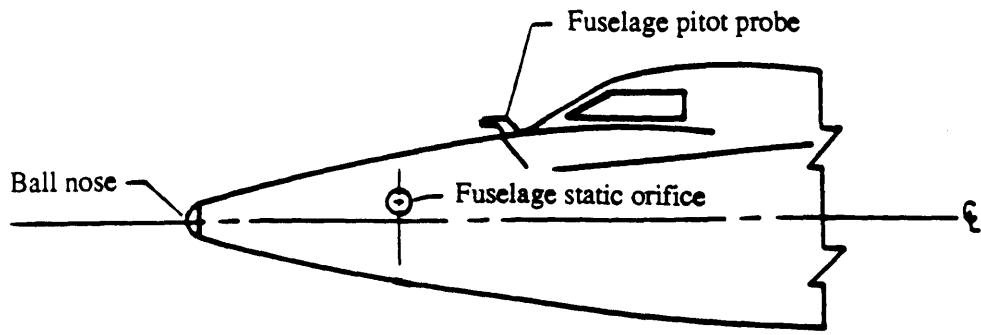


Fig 2.1.2 Schematic drawing of the X-15 ball nose sensor

taken from ref. 3 and 4

was rotated by a hydraulic actuator to face the streamwise direction by nulling the differential pressure between vertical and lateral pressure sensor pairs. The alignment angles of the sphere with respect to the aircraft reference axis indicated the angles of attack and of side slip. As shown in Fig. 2.1.2, the rear portion of the sphere contained the mechanical and electrical components. These components, along with the sphere, were cooled by vaporized liquid nitrogen. In order to test the thermal load and thermal transient on the ball nose sensor, a F-100 exhaust nozzle was placed in front of the X-15, and the ball nose sensor was exposed to high temperature up to 1200°F by hot after burner flame. The X-15 structure and associated components behind stagnation points were capable of withstanding temperatures of approximately 1200°F. The static pressure sensor was flush mounted on the side of the conic nose.

In Table 1, the achieved performance of the X-15 ball nose sensor system is summarized.^{3,4,5} Altitude was measured by ground tracking radar, and supplemented with Inertial Navigation System (INS) data. A 1% (1σ) accuracy was reported. Dynamic pressure was computed from the measurements of total pressure, static pressure, and Mach number, obtained from the Ball nose sensors. An accuracy of 5 - 10% was reported. Higher accuracy in dynamic pressure is reported at high Mach number where the uncertainties in static pressure and Mach number do not contribute significantly. The accuracy in angle of attack and side slip angle was $\pm 0.25^\circ$ as measured by the Ball nose system. Accuracy in angle of attack and side slip decreases as the dynamic pressure decreases. An accuracy of 1% was reported in the Mach number measurement with the pitot probe type sensor.

**AIR DATA MEASUREMENT PERFORMANCE
X-15 BALL NOSE SENSOR**

Performance		Range	
Angle of Attack	α	-5° +26° +26° +38°	±0.25°
Angle of Side Slide	β	±20°	±0.25°
Mach Number	M	0 - 7	1%
Dynamic Pressure	q_{∞}	20 - 2500psf	1.67% - 3.3%
Total Pressure	P_t	20 - 3000psf	
Static Pressure	P_{∞}	0 - 2100psf	0.33% - 0.67%
Altitude	h	0 - 350kft	±1% (INS)

Table 1

2.1.1 SENSOR PROBLEMS ENCOUNTERED DURING X-15 OPERATION

The flow direction parameters (α, β) were defined as the free stream flow direction with respect to the aircraft reference axis. Static alignment of the ball nose sensor with respect to the aircraft reference axis needed to be nulled out within order of magnitude smaller than the angular resolution of the sensor. Since the sensor was heavily dependent on moving mechanical parts such as the servo actuator, position sensor, and rotating sphere, the ball nose sensor was more susceptible to component failures than other air data systems. The servo with negative feedback often caused 4Hz and 12Hz limit cycle due to its rate limited servomechanism. At low dynamic pressures on the order of 40PSF and less with high angle of attack of 26° and higher, the collar of the spherical sensor housing caused flow interference, consequently a significant amount of error appeared in angle of attack measurement. During subsonic operation, up wash effects on the sensor caused the error in angle of attack and angle of side slip measurements. The fuselage static sensor is susceptible to large position error and sensitive to variations in angle of attack for Mach number greater than one; consequently, altitude and Mach number measurement was difficult.

2.2 SHUTTLE AIR DATA SYSTEM

The flight envelope of Space Shuttle, which consists of variations in Mach number between 0.3 and 27, angle of attack from -5° to 45° , and peak stagnation temperature up to 2000°F is analogous to the reentry phase of proposed airbreathing hypersonic vehicles. Three different types of air data system were used for the Space Shuttle. In the boost phase, a conventional pitot tube was mounted on top of the external fuel tank. During the

reentry, the fuselage mounted pitot probe is deployed at Mach number less than 3, and used for approach and landing. The Shuttle Entry Air Data System (SEADS) is designed for the reentry phase of the flight and used once on the Columbia Space Shuttle Orbiter. The SEADS was proposed as an air data system covering hypersonic flight regime. However SEADS was capable of providing necessary air data parameters from 250 Kft to touch down.¹⁴

The initial Space Shuttle air data system consisted of two conventional fuselage mounted pitot differential probes shown in Fig 2.2.1.² At Mach numbers lower than 3.5, the probes are deployed from the side of the fuselage. The probes were prohibited to use at higher Mach numbers due to high thermal load on the probe structure. The blunt body of the Space Shuttle causes substantial amount of position error in the fuselage mounted pitot probe and static pressure orifice when compared to the pitot-static boom system with the probe located few fuselage diameters away from the nose. The fuselage mounted pitot tube probes were calibrated by the supersonic wind tunnel tests and inflight tests to obtain the empirical calibration coefficients to account for the position error and the pressure jump during transonic flight.

The Shuttle Entry Air Data System (SEADS) is shown in Fig. 2.2.2.¹ The SEADS employed a cruciform array of 14 pressure transducers on the nose cap and 6 static orifices are located aft of the nose cap. The SEADS is based on the flush orifice concept. The nose of the Shuttle Orbiter functions as both pitot-static probe and flow directional sensor. Instead of the rotating sphere of the X-15, fixed flush orifice arrays were mounted on the forebody of the Shuttle as shown in Fig. 2.2.2. A computational technique supplemented with wind tunnel testing was used to extract air data parameters from the pressure field measurements. Extensive wind tunnel tests and inflight tests showed that the flush mounted pressure sensor system can be used from subsonic speed to hypersonic speed by creating

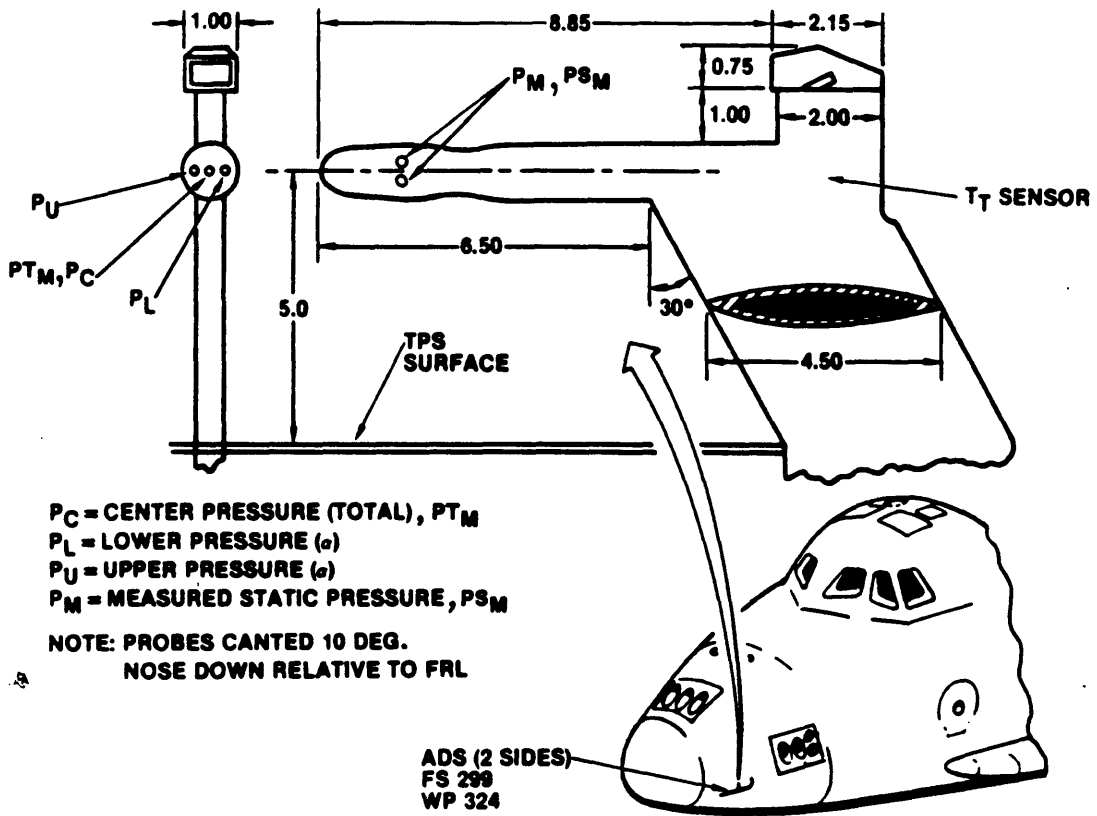


Fig 2.2.1 The Space Shuttle fuselage mounted pitot-differential probes

taken from ref 2

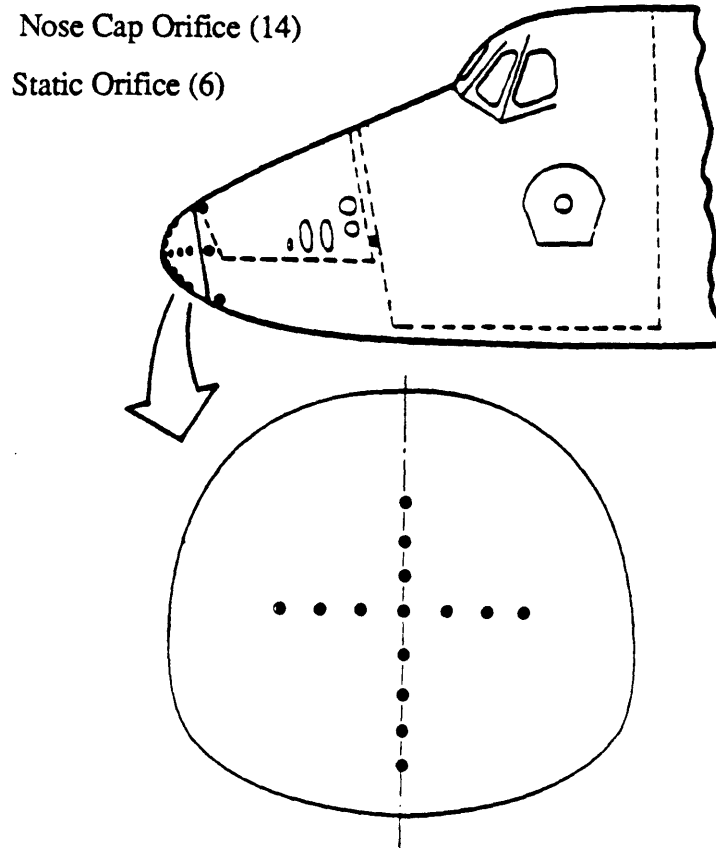


Fig 2.2.2 SEADS Orifice Configuration

taken from ref. 1

semiempirical flow model of the forebody and change the filter parameters as Mach number varies.

The thermal loads on the SEADS pressure transducers were relatively low due to the Space Shuttle thermal isolation tiles. The pressure transducers are buried deep inside the fuselage and wrapped with the thermal insulators. Due to good thermal insulation, the transducers operated near room temperature with less than 25°F increase throughout the reentry.¹⁵

Actual performance of the SEADS system from the Columbia Space Shuttle is unavailable at this time. In Table 2, the predicted performance of the Shuttle air data system is summarized.¹ The performance specification is based on the high speed Wind tunnel data.¹ Based on the predicted performance, the SEADS system is capable of providing total pressure measurement with $\pm 0.5\%$ uncertainty. Also, the predicted static pressure and Mach number measurement accuracy is within $\pm 5\%$ uncertainty. For supersonic speed, the predicted dynamic pressure measurement accuracy is within $\pm 3.3\%$ uncertainty. The sensor system is capable of providing flow direction parameters, angle of attack and side slip angle, with $\pm 0.25^\circ$ uncertainty.

**AIR DATA MEASUREMENT PERFORMANCE
SHUTTLE ORBITER**

		<u>Range</u>	<u>Required Accuracy</u>	<u>Actual Performance (WT Tests)</u>
Angle of Attack	α	-10°+45°	±0.66°	±0.25°
Angle of Side Slide	β	±6°	±0.66°	±0.25°
Mach Number	M	0 - 3.8	±5%	5.2%
Dynamic Pressure	q_{∞}	90 - 375 psf	±3.3%	3.3%
Total Pressure	P_t	0.5 - 2100 psf		0.5%
Static Pressure	P_{∞}	0.5 - 1900 psf		5%
Altitude	h	10kft-100kft 100kft-Orbital	±3.3%	
Vertical Velocity	h	0 - 600ft/s	±1.6%	
Free Stream Velocity	V_{∞}	0 - 3387ft/s	±0.984ft/s ±1.64ft/s	

TABLE 2

2.3 SR-71

The SR-71 uses a conventional pitot-static nose boom air data system similar to the X-15 nose boom sensor. The most interesting instrumentation requirement came from the propulsion control system. The SR-71 employs active inlet control and uses surface pressure measurement to estimate the normal shock location inside the engine inlet. The engine inlet control system provide insight of the inlet pressure measurement accuracy and bandwidth requirements. Both air data and propulsion control systems are discussed in next section.

2.3.1 SR-71 AIR DATA SYSTEM

The SR-71 is a Mach 3+ reconnaissance aircraft which employs a high quality conventional pitot-boom type air data system. Because of its relatively low Mach number operation, a conventional pitot-static boom probe is mounted on the tip of the nose. The probe is extended a few fuselage diameters away from the nose in order to reduce the position error caused by the fuselage. In Table 3, the conventional pitot-static probe performance, SR-71 is summarized.⁷ In general, the system provided less accurate data during the transonic region due to the large irregular pressure jumps. Mach number is measured with an uncertainty of ± 0.012 at supersonic cruise and ± 0.004 at subsonic cruise. The SR-71 which cruises at the trim angle of attack of 5° , has angle of attack and side slip uncertainties of $\pm 0.25^\circ$. Angular uncertainties double during transonic flight phases. The dynamic pressure uncertainty of ± 1.5 PSF at supersonic flight increased to ± 6 PSF during the subsonic flight due to the fact that the dynamic pressure is an inferred parameter which relies on the total pressure, static pressure, and Mach number

AIR DATA MEASUREMENT PERFORMANCE

SR71

			<u>Range</u>	<u>Performance</u>
Angle of Attack $\pm 0.25^\circ$	α	Sub/Supersonic Transonic		$\pm 0.5^\circ$
Angle of Side Slide	β			$\pm 0.25^\circ$
Mach Number	M	Supersonic Subsonic	0 - 3.5	± 0.012 ± 0.004
Dynamic Pressure	q_∞	Supersonic Subsonic		± 1.5 psf ± 6 psf
Altitude	h	Sub/Supersonic Transonic	0 - 80kft	± 151 ft ± 220 ft
Free Stream Velocity	V_∞	Supersonic Subsonic	0 - 3400ft/s	± 1 ft/s ± 1.7 ft/s

TABLE 3

measurements. The significance of the static and Mach number uncertainties increases at low Mach numbers. The SR-71 has a maximum ceiling of approximately 80 Kft. and the ADS can provide the altitude data within ± 150 ft during supersonic and subsonic flight. The error in altitude increases during the transonic region to ± 220 ft due to the pressure jump effect.

The high temperature air data sensor system is needed for the SR-71 due to its hot structure configuration. The air data sensors are required to withstand 900 deg F heat loads. In order to minimize the thermal effects on the air data pressure transducers, the air data pressure transducers are installed inside the thermally stabilized instrument case and long pneumatic lines are used to connect the pitot-static nose boom and the transducers.

2.3.2 SR-71 PROPULSION CONTROL SYSTEM

Engine control on the SR-71 is important at supersonic speed.⁶ The SR-71 employed a mixed-compression supersonic inlet to decelerate the inlet flow from supersonic to subsonic without large pressure loss (i.e. engine efficiency loss). The inlet section is shown in Fig. 2.3.1. At normal stable condition, supersonic flow is decelerated as it goes through several weak oblique shocks between the translating center-body and axisymmetric inlet. When the flow decelerated to near Mach 1, it goes through a normal shock in just aft of the throat where the cross section area is minimum. An unstarted condition occurs when the normal shock jumps to the throat area or forward of the throat area the pressure then builds up inside the engine and creates a strong shock wave in front of the inlet as shown in Fig. 2.3.3. The combustion goes out and results in unstart. Such large drag on one of the two wing mounted engines caused the aircraft to go out of control.

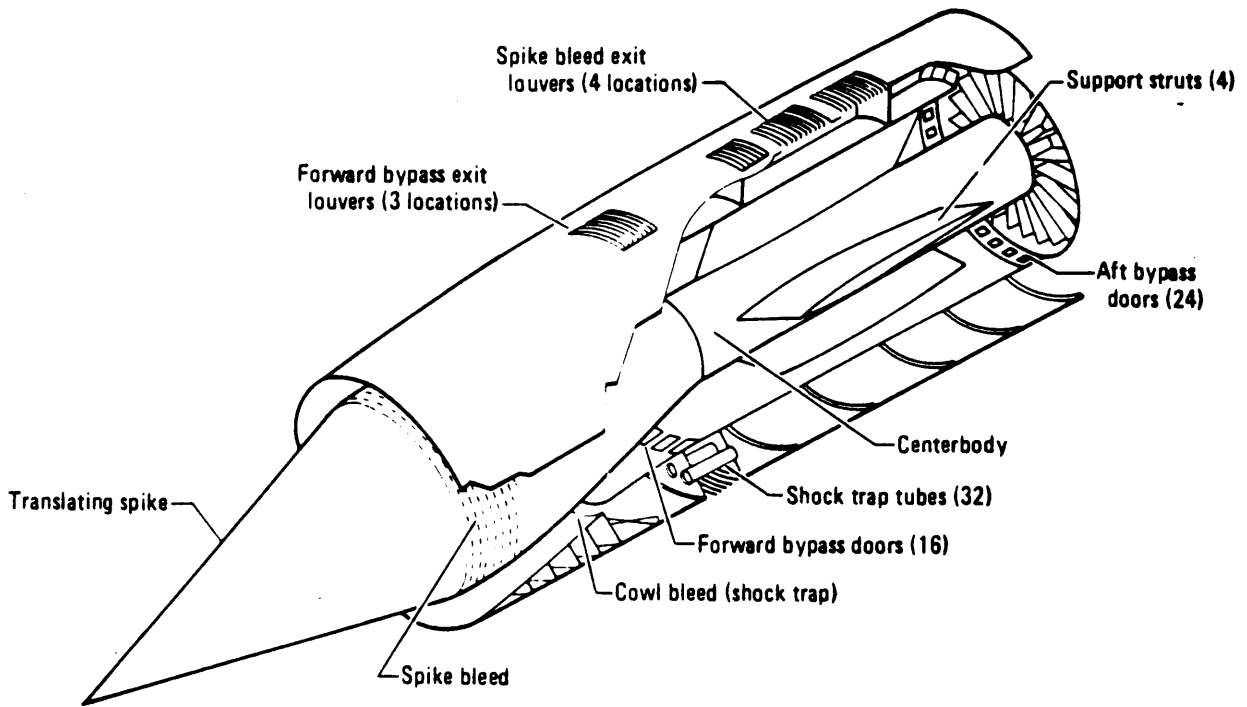


Fig 2.3.1 Cutaway view of the SR-71 inlet

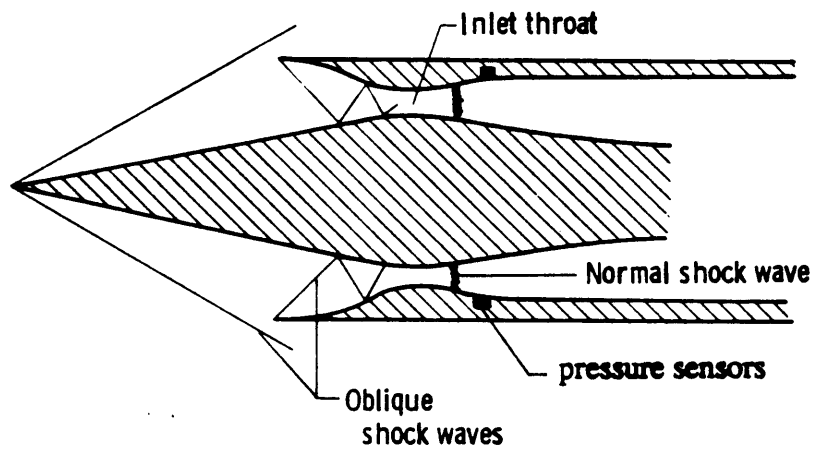
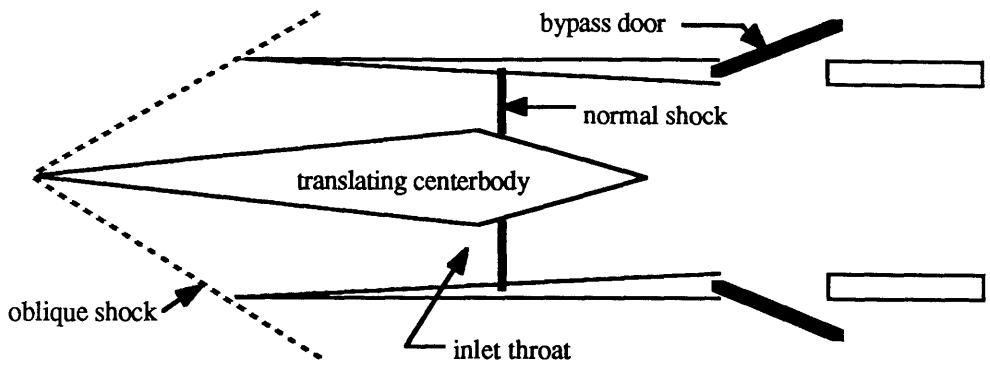
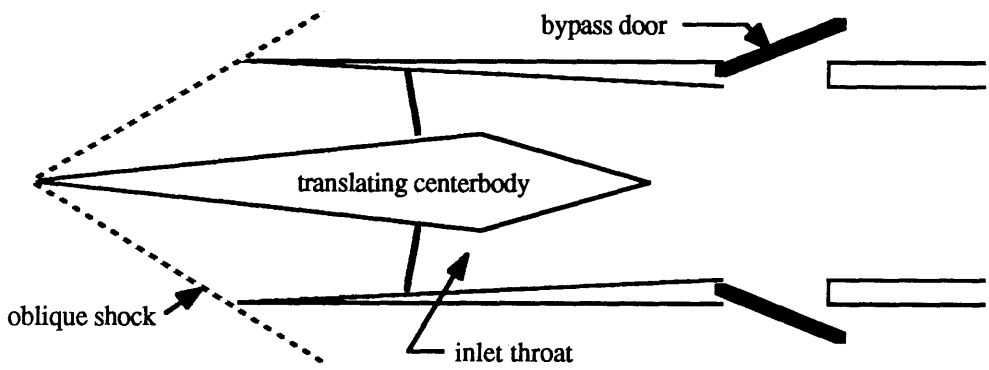


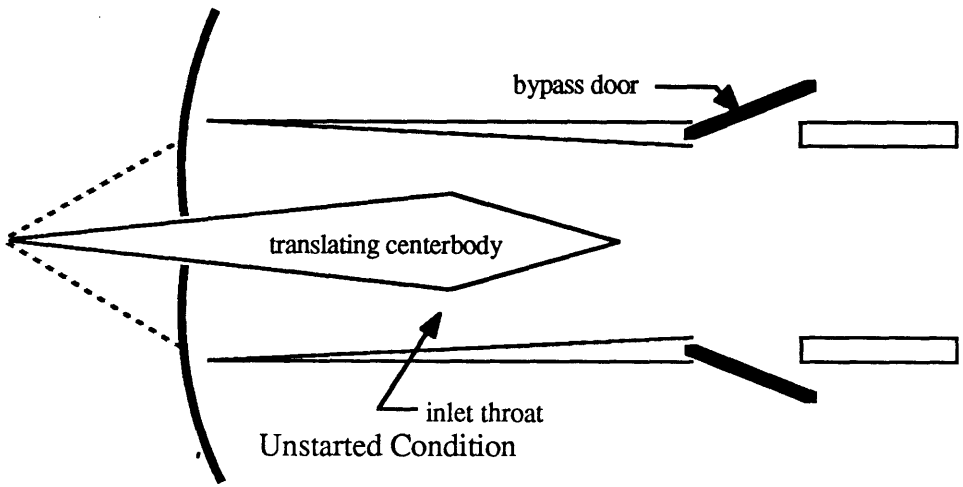
Fig 2.3.2 Shock system associated with mixed-compression inlet and the inlet pressure transducer location



Nominal Operation



Beginning of Unstart



Unstarted Condition

Fig. 2.3.3

The SR-71 employed an active compression cone, flow dumping bypass door, and inlet surface pressure sensors to control the shock position inside the axisymmetric inlet shown in Fig. 2.3.1. A compression cone inside the inlet moves in the streamwise direction to keep the first shock near the critical condition which is the condition where oblique shock is attached at external circular cowl lip and the normal shock is aft the throat, and maximize the mass flow rate. Flow dumping bypass doors are used for high bandwidth control of the normal shock location. The SR-71 employed pressure sensors at aft of the throat exit to determine the normal shock position (Fig. 2.3.2). A Linear Quadratic Gaussian Optimal Regulator scheme is used to maintain a stable shock position in the presence of random flow disturbance and sensor noise.

The sensor specifications for the inlet control consist of the nominal operating pressure of 5400 PSF and about 1500° F with accuracy about 0.1%. During the supersonic cruise phase, the throat exit static pressure was 5400 PSF and the flow disturbance measurement was 54 PSF rms. The sensor therefore had to be temperature compensated. The measurement noise (sensor noise) must be low in order to have high open loop gain for good DC performance. Also phase lag and time delay of the sensor orifice should be minimized and/or the phase information should be known in order to stabilize the control loop.

The SR-71 propulsion control system required a wide bandwidth pressure sensor system (up to 500 Hz).¹⁵ The pressure sensor bandwidth requirements are determined by the inlet dynamics ($G(s)_{inlet}$) and the bypass door control dynamics ($G(s)_{bypass}$). The sensor bandwidth should be much wider than the bandwidth of the controller and inlet dynamics. The SR-71 propulsion control system block diagram is shown in Fig. 2.3.4. The bode plot of the inlet dynamics is plotted in Fig. 2.3.5 from the data in reference 6. The inlet dynamics are the response of throat exit static pressure with respect to the input of the

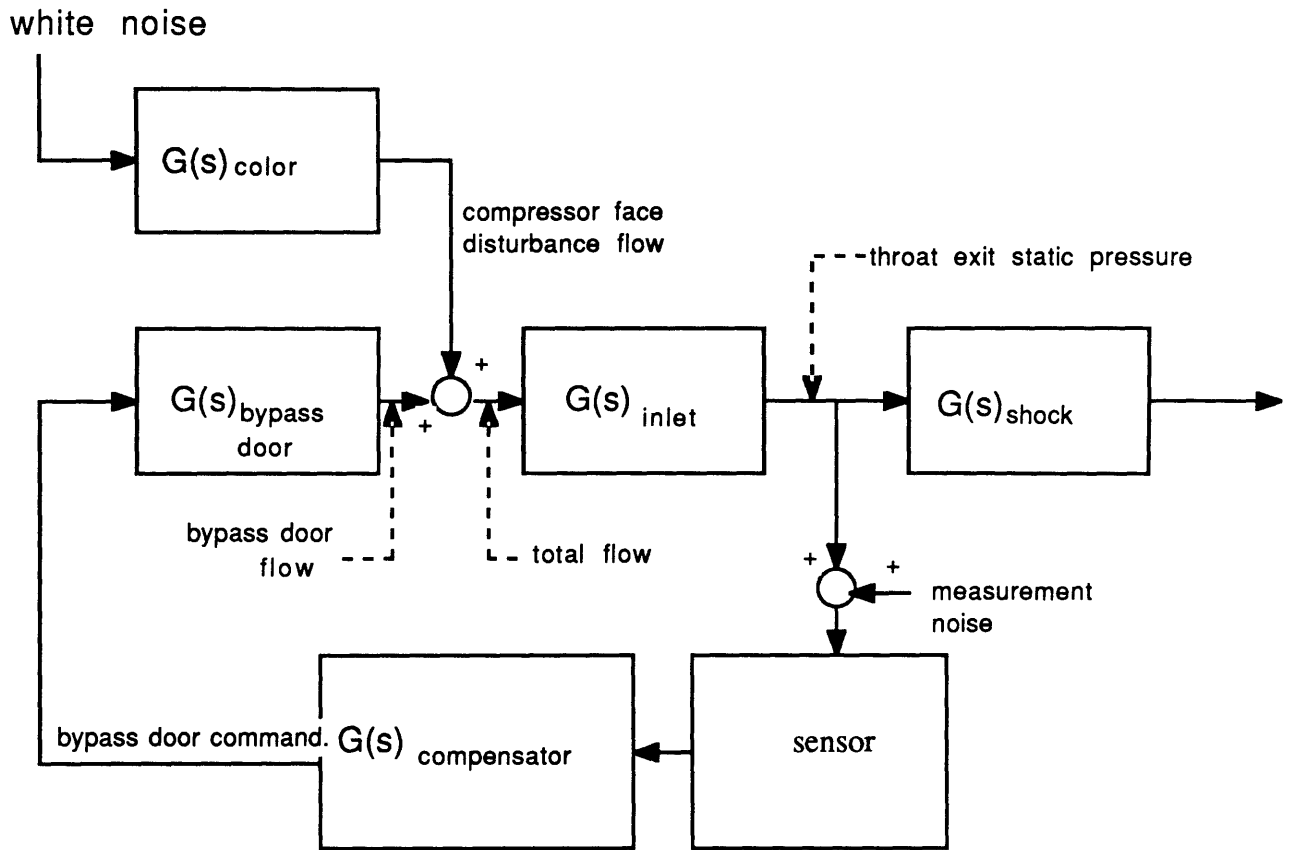


Fig. 2.3.4 SR-71 Inlet Control System

compressor face disturbance flow and the bypass door flow. The inlet dynamics have a bandwidth of well over 80Hz. The bode plot of the bypass door dynamics (i.e. the controller dynamics) is plotted in Fig. 2.3.6. The bypass door control dynamics are the response of bypass door flow with respect to the bypass door command from the Kalman filter and the compensator dynamics. The bandwidth of the controller was about 120Hz. Usually the bandwidth of the control acutators(in this case it would be the bypass door mechanism) is the limiting factor for the sensor bandwidth requirement, however, the SR-71 bypass door bandwidth was about the same as the plant bandwidth. In a conservatively rated control system, the sensor bandwidth should be 5 to 10 times the controller and plant combined dynamics bandwidth; therefore the required sensor system bandwidth was about 500Hz.

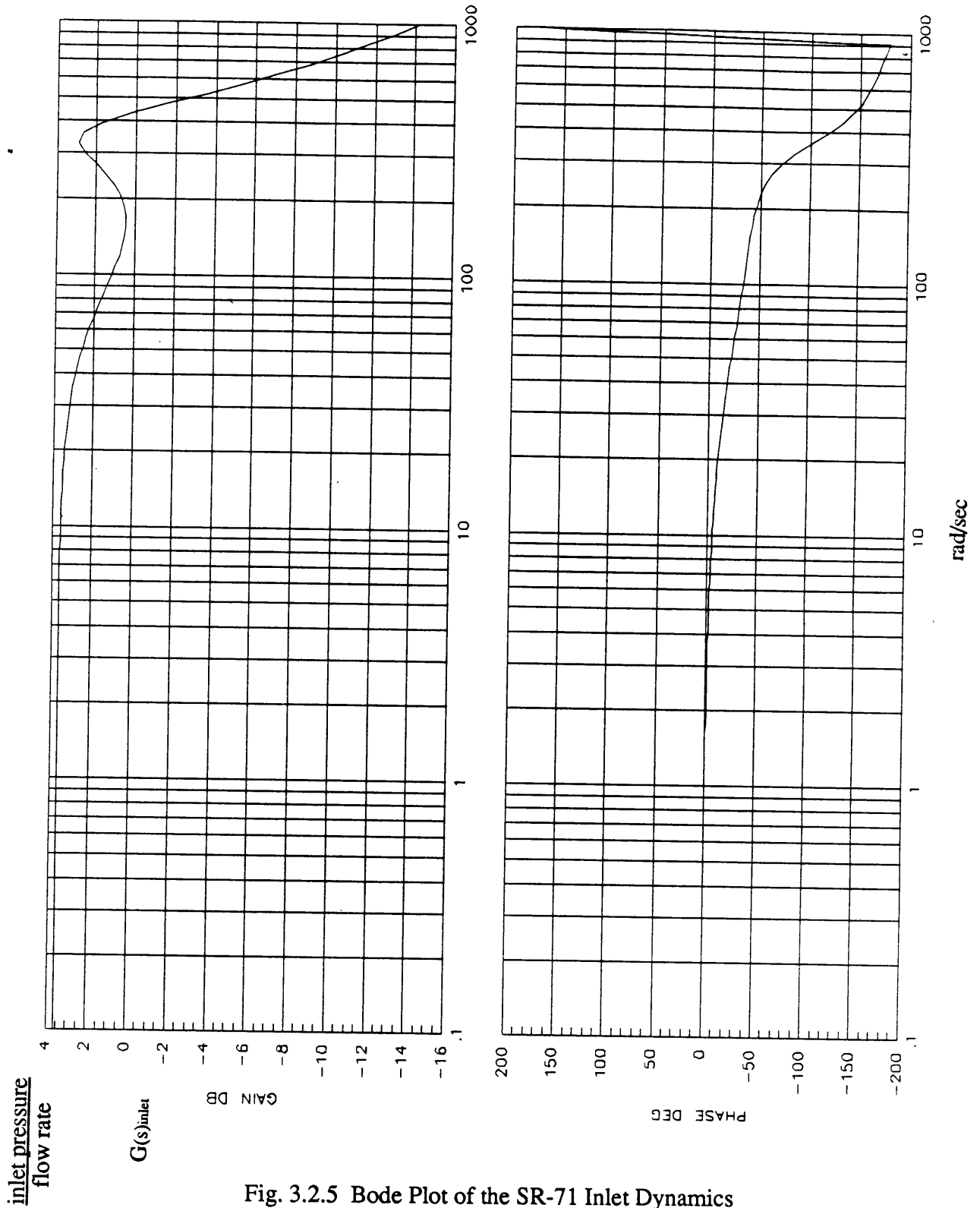


Fig. 3.2.5 Bode Plot of the SR-71 Inlet Dynamics

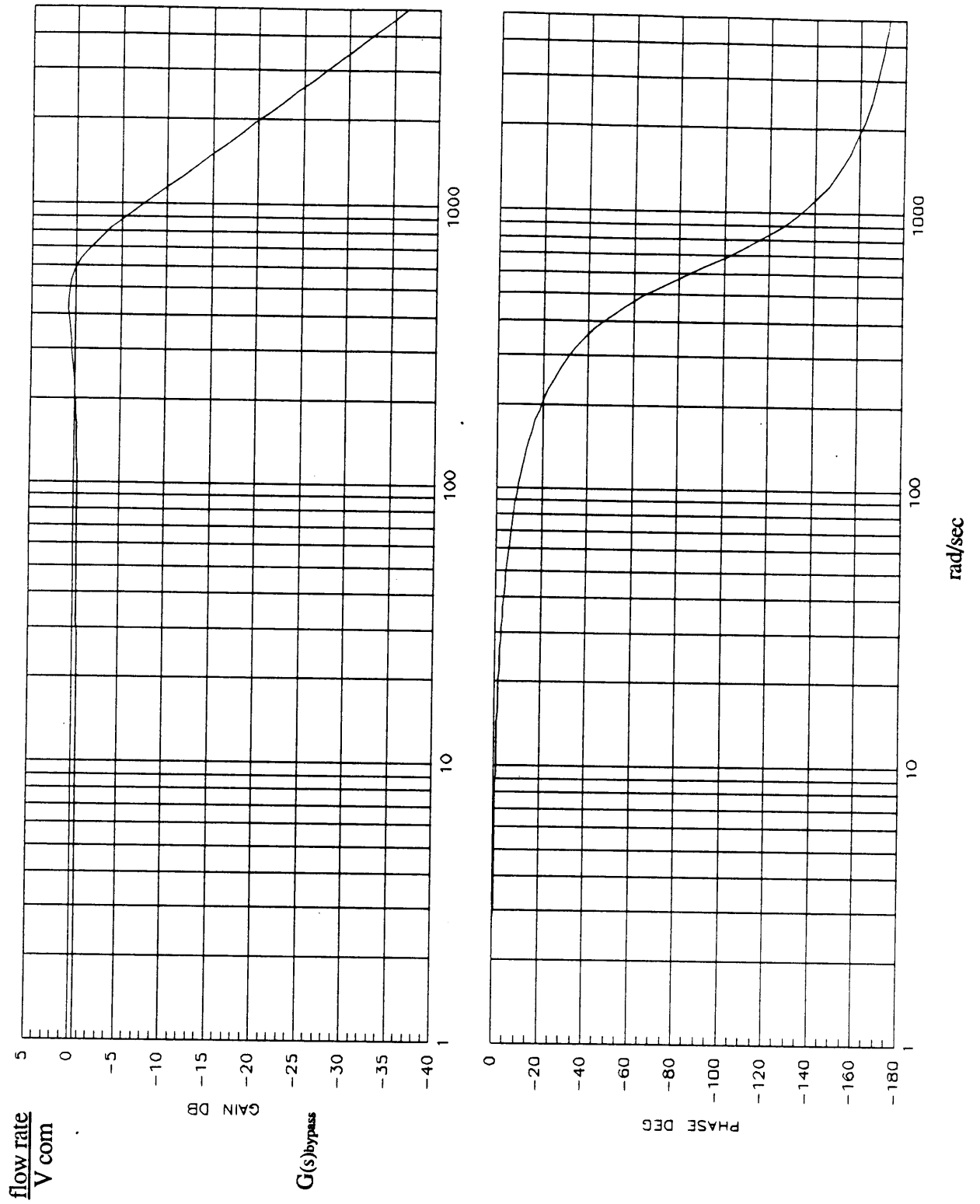


Fig. 3.2.6 Bode Plot of the SR-71 Bypass Door Dynamics

3.0 PROJECTED SENSOR ENVIRONMENT

In the process of defining the instrumentation requirements for hypersonic vehicles, the following assumptions are made. The main flight phase of interest is assumed to be the hypersonic cruise phase in the air-breathing engine corridor. The vehicle is assumed to employ both the ramjet and scramjet during the cruise phase. The vehicle configurations and the flight corridor determine the sensor environment.

The hypersonic vehicle configurations are discussed in next section based on available information of potential NASP configurations. Also, the flight trajectory and vehicle environment are discussed in order to define the environment in which the sensors has to operate.

3.1 HYPERSONIC VEHICLE DESCRIPTION

Hypersonic cruising vehicles may be categorized in two different configurations, low hypersonic Mach number ($M < 6$) cruising aircraft and transatmospheric vehicles. Low hypersonic Mach number cruisers such as the "Orient Express", are proposed as a high speed long range transport aircraft. By employing air breathing engines, which eliminate the disadvantages of turbojet limitation and inefficiency of rocket, efficient high speed flight would be obtained.

Another application would be the air breathing transatmospheric vehicle. There are many proposed configurations of the transatmospheric vehicles such as the National Aerospace Plane (NASP), Sanger, and HOTOL. The NASP(Fig. 3.1.1) is proposed as a single stage, horizontal take off, airbreathing, transatmospheric, launch vehicle. The Sanger is proposed as a two stage launch vehicle where a mother ship employs air

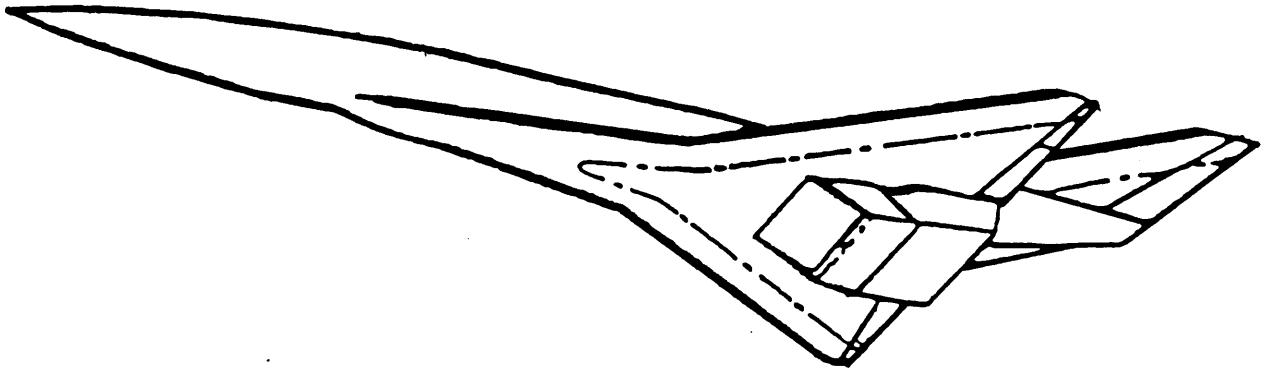


Fig 3.1.1 NASP

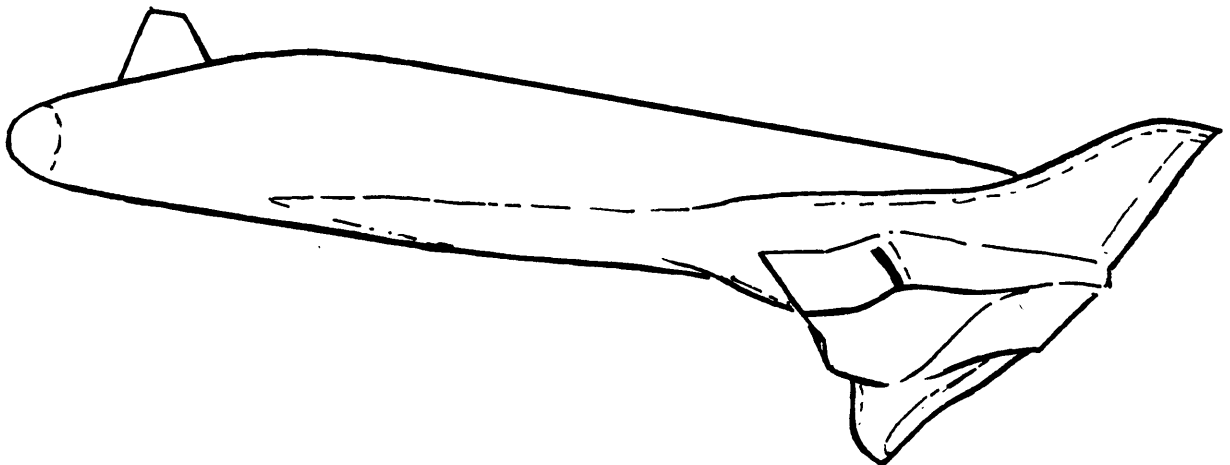


Fig 3.1.2 HOTOL

breathing engines to accelerate the second stage to a high Mach number then returns to base. The second stage then uses rocket thrust to obtain orbital velocity. The HOTOL(Fig. 3.1.2) is proposed as a single stage orbiter which uses special airbreathing engines to accelerate up to Mach 5, then uses rocket engines to obtain orbital velocity.

The common elements of the above vehicles are that the hypersonic vehicles would employ air breathing engines and fly at very high Mach numbers through atmosphere in aircraft like configurations. The major instrumentation requirements would come from the vehicle flight control system and the air-breathing propulsion control system.

3.2 POTENTIAL CONFIGURATIONS

A typical hypersonic cruise transatmospheric vehicle has several unique features which result from it's rigorous functional requirements. The conceptual NASP vehicle schematically shown in Fig. 3.2.1, which functions as both a reentry vehicle and hypersonic cruiser, will have a highly swept and low aspect ratio wing which will be integrated with the aircraft fuselage in a lifting body configuration. In the hypersonic flight regime, drag is a function of frontal area, fuselage surface area, and thickness ratio square; consequently, slender body configuration is required for efficient flight. The vehicle will likely cruise with the airbreathing engines located under the fuselage. The slender forebody functions as the inlet compressor and guides the flow into the airbreathing engine. Variable inlet geometry and combustor height adjustment are highly desirable. Both ramjet and scramjet configurations may be used. Much of the current design consideration is focused on the thermal limitations which result from the high speed flight, and high speed flow combustion constraints.

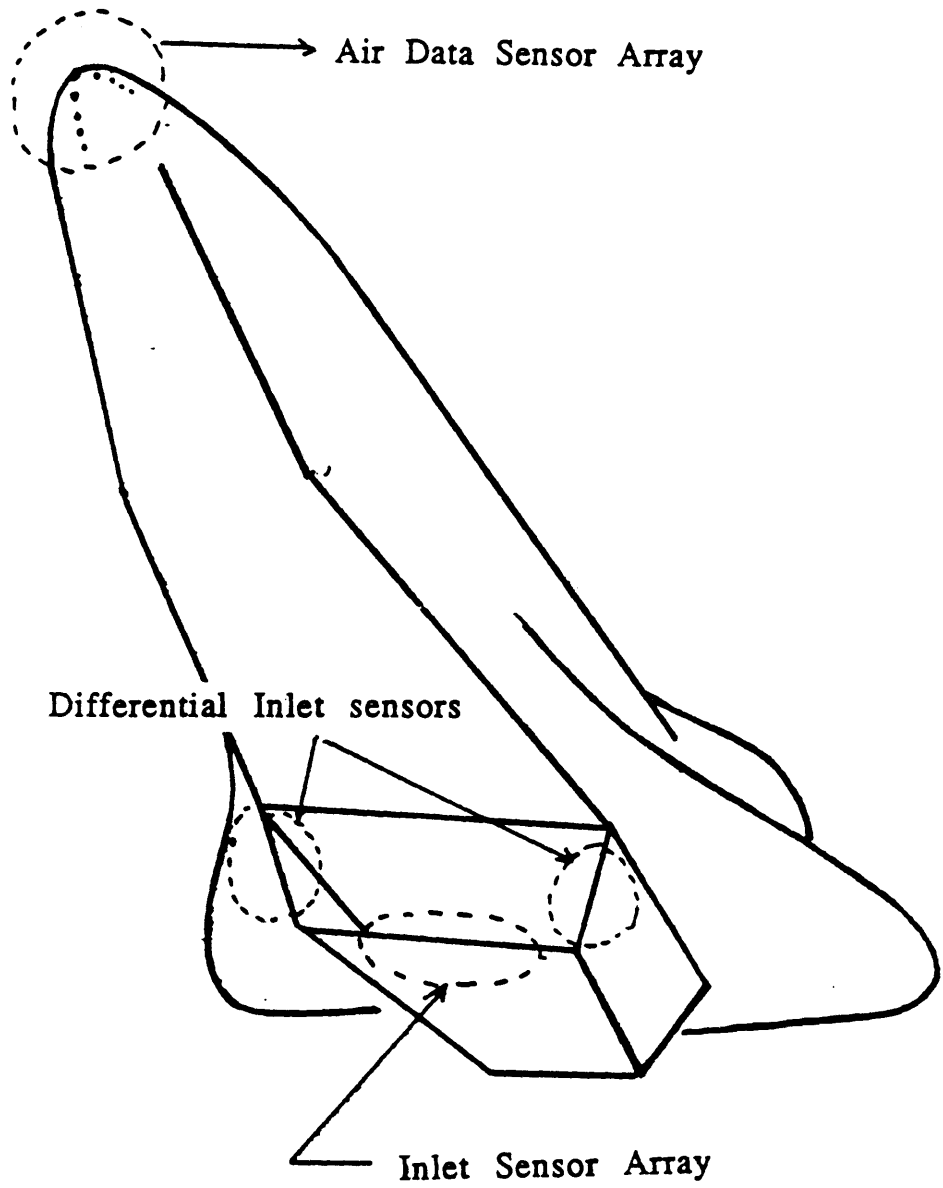


Fig 3.2.1 Potential Pressure Sensor Locations

Due to the thermal problems associated with the high Mach number flight, the airbreathing hypersonic vehicles will likely employ non-intrusive air data sensors on the forebody (Fig. 3.2.1). The tip of the vehicle nose is the most desirable location because the flow direction parameters (α, β) can be measured more accurately since the errors in flow direction, which are caused by fuselage disturbance, are minimum at the tip of the nose. Also, total pressure measurement requires the sensor to be placed on the stagnation point aft of the shock on the forebody. The measurement of propulsion parameters would likely be done by the sensors located on and inside the airbreathing engine inlet as shown in Fig. 3.2.1. For the ramjet operation, the normal shock location detection sensors would be located aft of the throat area. For scramjet operation, the inlet shock geometry detection sensors, inlet pressure sensors, and inlet temperature sensors would likely be placed inside the inlet aft of the oblique shock.

3.3 FLIGHT ENVELOPE

A single stage to orbit vehicle will likely have two distinctly different flight phases, ascent and reentry. The hypersonic vehicle will take off horizontally and accelerate to and cruise at hypersonic velocities through the airbreathing corridor shown in Fig. 3.3.1. The lower part of the airbreathing corridor shown in Fig. 3.3.1 is preferred for engine efficiency however heat loads will increase at lower altitudes. In reentry, the hypersonic vehicle will initiate deceleration at a high angle of attack in a manner similar to the shuttle reentry trajectory shown in Fig. 3.3.1. This is followed by high altitude and terminal area energy management maneuvers ending with a conventional runway landing. The hypersonic cruise phases pose the most stringent requirements on the air data and propulsion control systems due to the tight constraints on the flight and propulsion control systems and the difficult measurement environment.

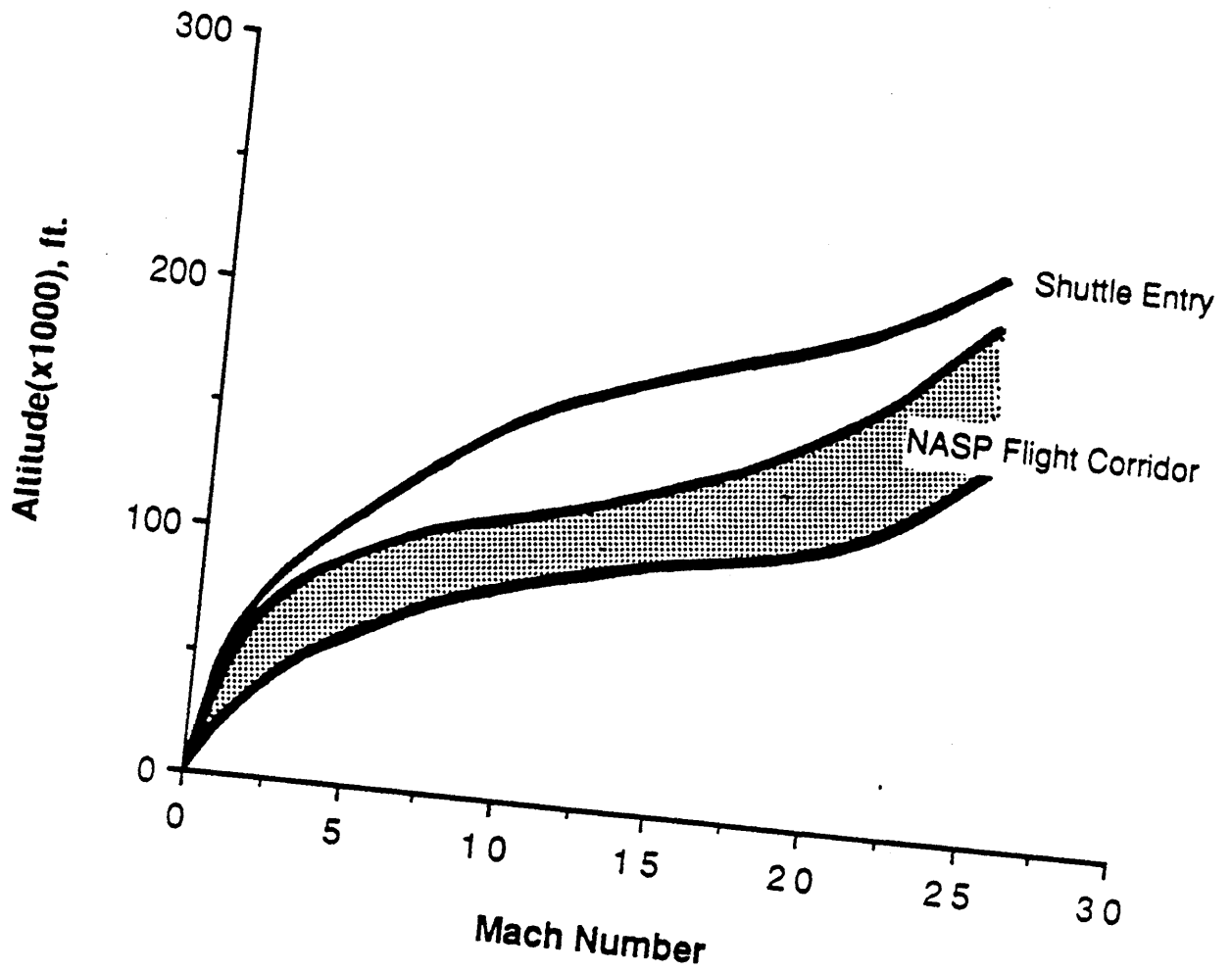


Fig 3.3.1 NASP and Space Shuttle (altitude, Mach number) trajectory

3.4 SENSOR ENVIRONMENT

As mentioned above, the desirable location for the air data sensors will be at the stagnation region of the nose. The inlet flow sensors would likely be located on the cowl lip region. These are likely to be the hottest region on the vehicle and the harsh environment imposed on the surface will dictate the sensor environment.

Based on the airbreathing corridor, the hypersonic vehicle will experience dynamic pressures of up to about 6000 PSF (3 atm) as shown in Fig. 3.4.1, however the vehicle will likely be cruising at maximum dynamic pressure of 2000 to 4000 PSF due to structural limitation. Stagnation temperature of up to 3000°F are considered possible. The stagnation temperature limit will be set by material thermal limitations. Also, high integrated heat load is anticipated since the vehicle is expected to cruise hypersonic for time periods of up to 2 hours.⁸

Due to the high temperatures, the stagnation regions will experience real gas effects during most of the flight.¹⁶ As indicated in Fig. 3.4.2, the high speed flow around the vehicle goes through the excitational vibration and finally undergoes dissociation at $M > 10$. Any measurement of air data parameters based on ideal gas properties would therefore have significant error due to real gas effect at $M > 10$. For example, in the hot stagnation point, the specific heat of the real gas will be smaller than the ideal gas case. Those air data parameters such as dynamic pressure which rely on assumed value of specific heat will result in gross errors if the specific heat changes are not considered.

The peak external surface temperature and the integrated heat loads inside the vehicle will dictate the sensor thermal requirements. The vehicle skin temperature is limited

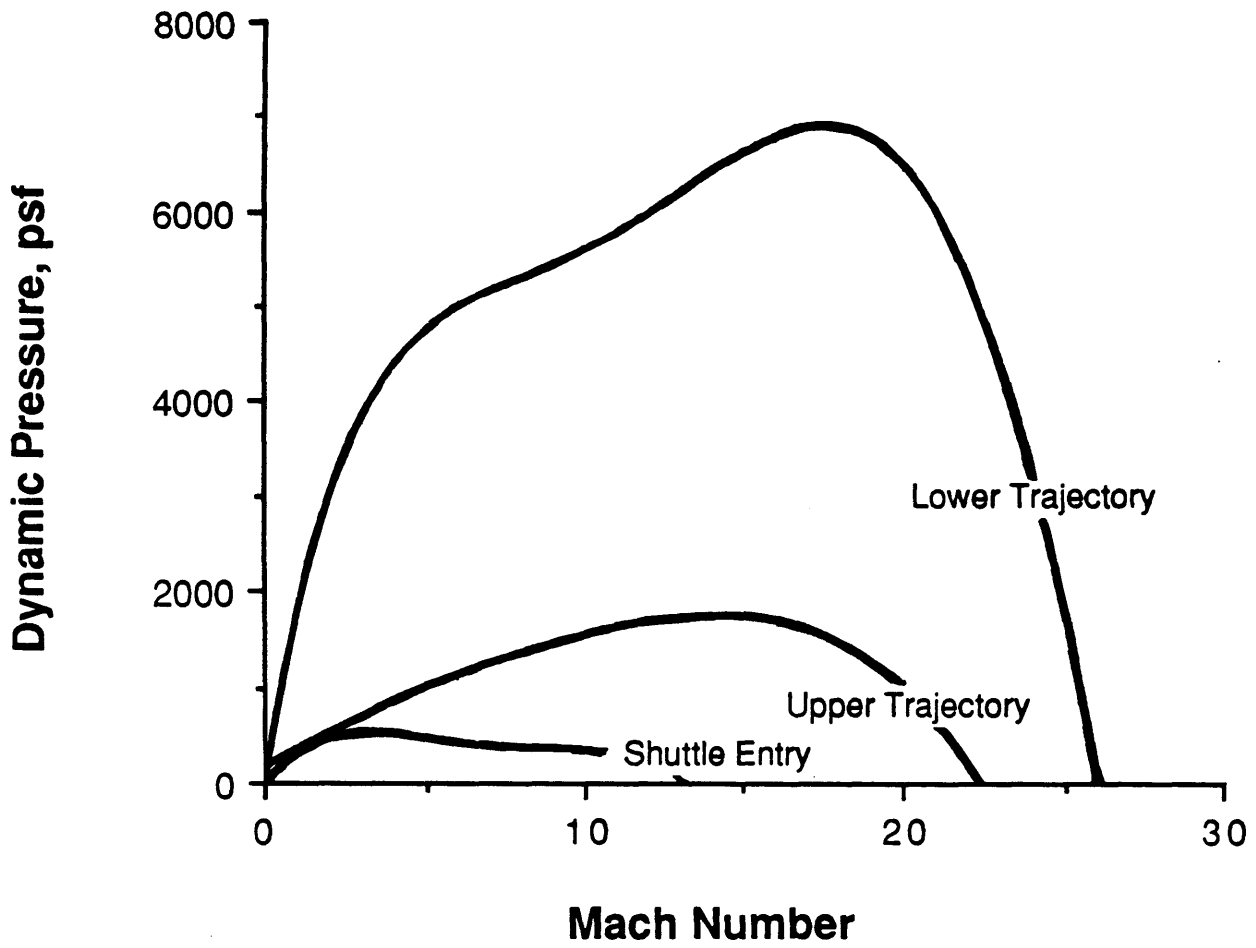


Fig 3.4.1 Dynamic Pressure vs Mach number

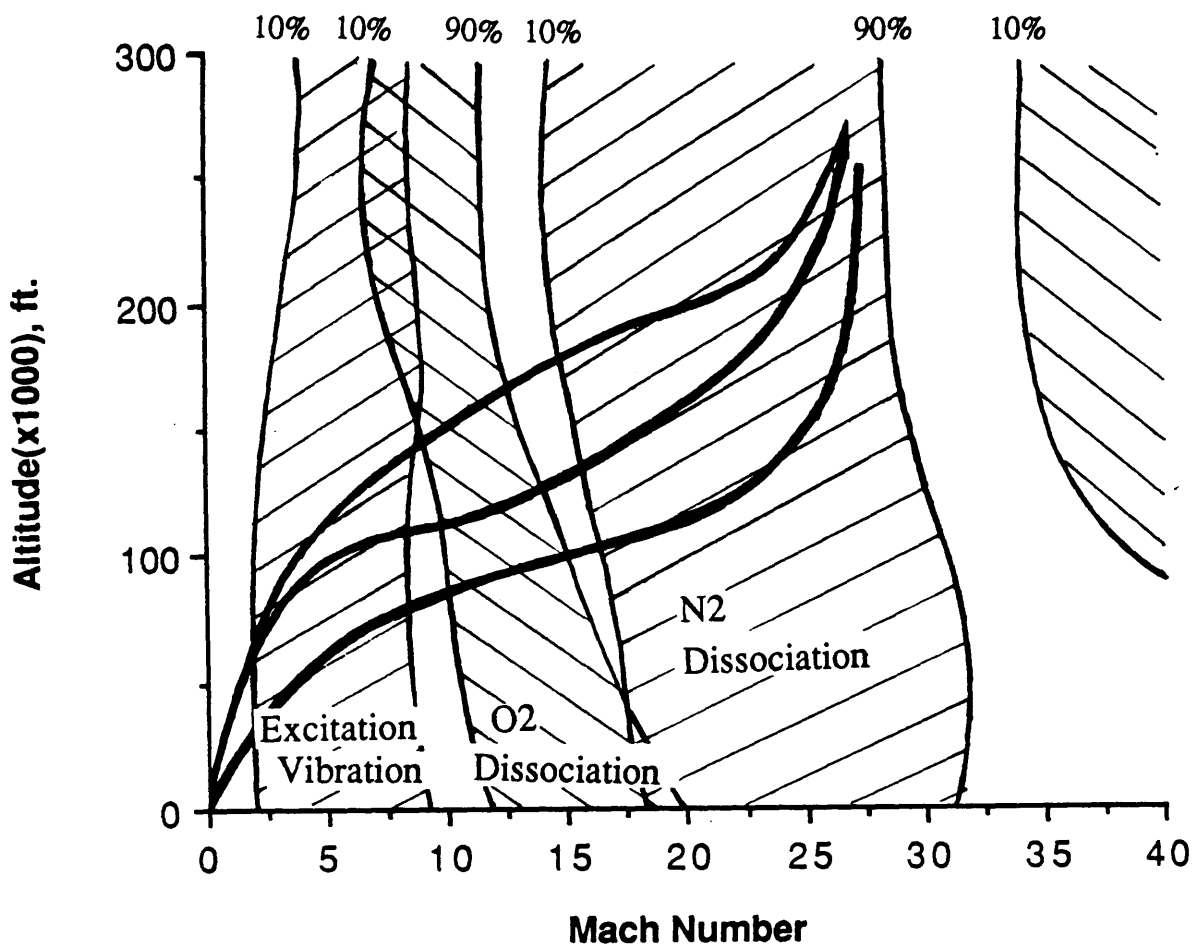


Fig 3.4.2 Stagnation Point Energy Excitation Zones

by the maximum temperature of the surface structural materials. Materials requirements may require an active cooling to prevent thermal destruction of vehicle fuselage. The integrated heat loads inside the vehicle will be dictated by the skin insulator materials and the exposure time. If the vehicle uses thermal tiles on the surface similar to the Shuttle; and long pneumatic tubes are used between the orifice and the transducers such as SEADS, high temperature exposure would be restricted to the orifice opening and the pneumatic lines. The thermal environment of the transducers would therefore be the vehicle internal equilibrium temperature. On the other hand, if the vehicle has a hot structure configuration (with or without surface cooling) and the required sensor systems are closely coupled to the surface, the thermal loads on both the orifice and the transducer will be very high.

4.0 THE INSTRUMENTATION REQUIREMENTS IMPOSED BY THE FLIGHT AND PROPULSION CONTROL SYSTEM

4.1 OVERVIEW

Air data measurements are needed by both the flight control system and the propulsion control system. The air data measurement requirements can be defined by analyzing the hypersonic vehicle flight and propulsion control requirements. The most unusual requirements come from the fact that the propulsion control system must be closely integrated with the flight control system because the airbreathing engines require a narrow range of angle of attack and side slip during hypersonic cruise in order to optimize propulsion efficiency. The air data system will function simultaneously as part of both the flight and propulsion control systems. In the next section, the functional measurement requirements for the flight control systems and the propulsion control systems are described.

4.2 FLIGHT CONTROL SYSTEM

The air data parameters which are required by the Navigation, Guidance and Control system, throughout the flight trajectory are:

- 1) Angle of Attack
- 2) Angle of Side Slip
- 3) Mach Number and Velocity
- 4) Altitude
- 5) Altitude Rate
- 6) Dynamic Pressure

The most stringent angle of attack measurement requirement comes from the hypersonic cruise phase. Angle of attack hold and pitch control may be needed due to stringent requirements from the propulsion control system which are described in next section. Angle of attack feedback is highly desirable to influence the short period mode of the vehicle. However implementation is extremely difficult because the control system requires extremely high quality measurements of angle of attack and angle of attack rate.

In a similar manner, angle of sideslip is needed to control the vehicle in a trimmed condition. Maintaining the vehicle in near zero side slip condition is also important because of the engine considerations which are described in next section.

Altitude measurement, (normally pressure altitude) is also needed for Inertial Navigation System (INS) stabilization. The INS is inherently unstable in altitude and altitude correction by either pressure altimetry or radar altimetry is needed. Mach number and altitude measurement is required to navigate the vehicle in desired air-breathing trajectory described in section x. Deviation from the designed trajectory would result engine unstart or excessive thermal or structural loads.

4.3 PROPULSION SYSTEM

The air data parameters and propulsion parameters are required to control the airbreathing engines. The most interesting feature of the proposed hypersonic vehicle is the scramjet operation.

The unknown flight regime occurs for flight Mach numbers between 6 and 25 where the scramjet propulsion system would operate. Scramjet operation through a wide spectrum of Mach numbers suggest that active control of inlet and nozzle geometry and

combustor height is needed. The optimal engine configuration may involve shock matching, inlet size, and compression ratio control which will depend on the flight Mach number. The feasibility of such active control is still unknown, however, following scramjet analysis is based on the engine configuration with variable geometry control.

In order to estimate the air data and propulsion state measurement requirements, important scramjet concepts are reviewed and the relationship between the vehicle attitude and the scramjet performance is explained below.

4.3.1 SENSITIVITY OF SCRAMJET COMBUSTION TO THERMODYNAMIC FLOW CONDITIONS

The scramjet is a very simple airbreathing engine configuration. High Mach number flow is decelerated to slower supersonic speed and then heat is added to increase enthalpy. The most important parameters are temperature, pressure, flow field, and mass flow rate into the combustor. The measurement of these propulsion parameters are required to control the scramjet. Variable geometry inlet and nozzle, variable combustor height, etc, are needed to control and provide adequate combustor thermodynamic condition.

According to recent investigation on the scramjet engine performance by Lewis M.¹³, combustor inlet temperature must be low enough to add heat to the flow and increase enthalpy. At sufficiently high temperature, added fuel will dissociate. The dissociation will absorb energy and result in a net loss of heat from the flow. On the other hand, combustor inlet temperature must be high enough to create spontaneous combustion. In the Fig. 4.3.1, hydrogen combustion time is plotted against pressure and temperature. At relatively low temperature of 900 to 1000°K, secondary reactions within the hydrogen-air

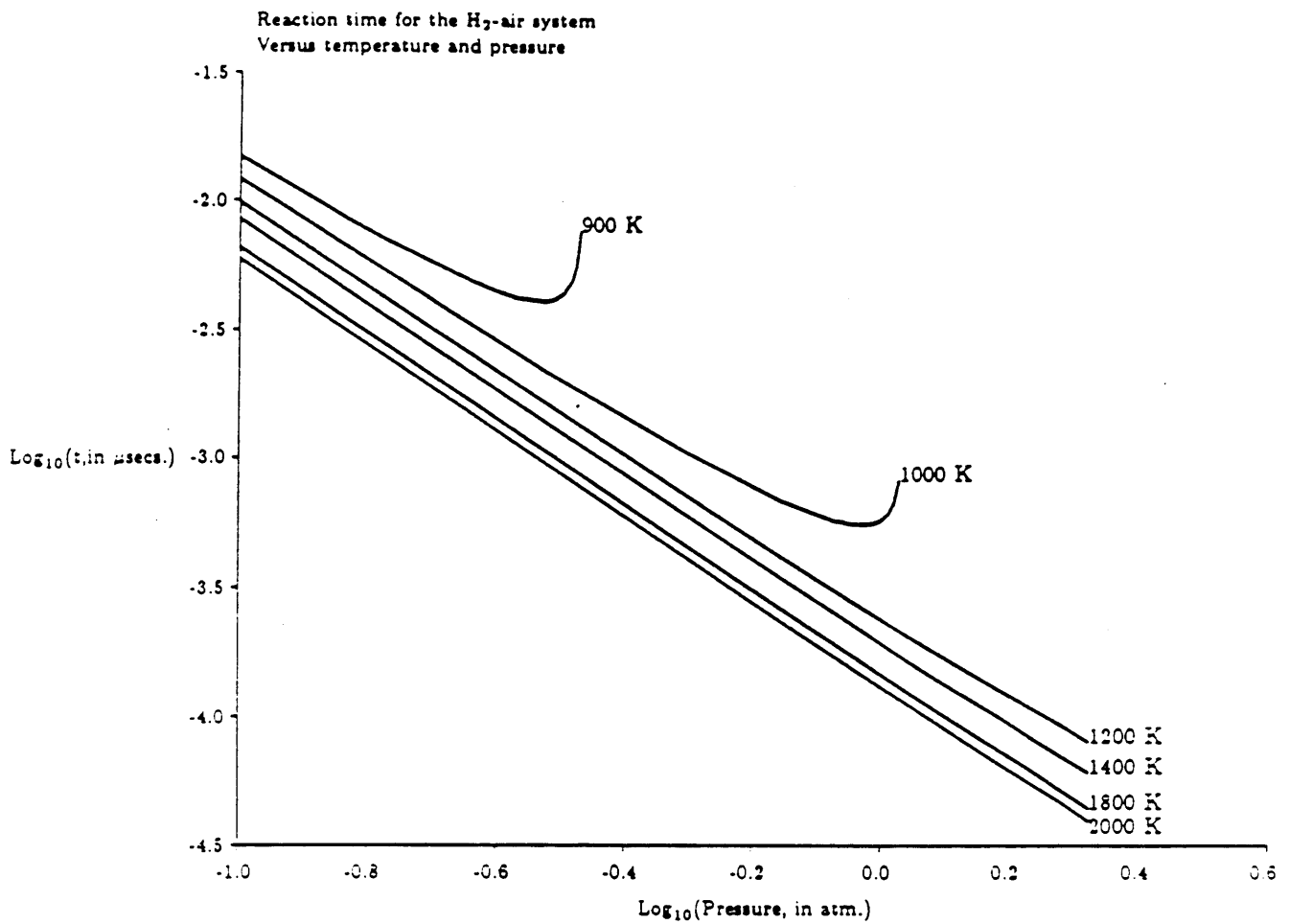


Fig 4.3.1 Time for completion of hydrogen combustion in air

taken from ref.13

system decrease combustion as pressure increases past cutoff value. Flame dislocation and combustion time delay are computed to be negligible even at the extreme cases since hydrogen is a such fast reacting gas. Therefore flame dislocation and combustion time delay can be ignored in propulsion control.

Heat addition rate is more sensitive to combustor inlet pressure than temperature. In general, reaction time decreases as pressure increases. Consequently, combustor inlet pressure must be as high as structure can withstand to maximize combustion efficiency. The inlet pressure should be high in order to take large amount of mass flow without high drag penalty from a large inlet. However, at lower temperature, pressure must be kept below the cutoff pressure where the secondary reactions start. Therefore it is important to keep the pressure and temperature within narrow range. The inlet values must be measured in order to control the combustion process.

The flow Mach number in the combustor is another important parameter. Inlet efficiency (i.e. total pressure recovery) will increase if the inlet flow deceleration is low. However, burning fuel at high Mach number results in higher total pressure penalty in the combustor.¹³ Therefore a compromise must be made between inlet and combustor condition for the optimal engine efficiency.

4.3.2 SENSITIVITY OF COMBUSTION TO VEHICLE ATTITUDE AND TRAJECTORY

Along with the free stream conditions, the inlet shock geometry determines the combustor thermodynamic condition. The shock geometry is directly related to the vehicle attitude and flight trajectory as well as the engine inlet geometry which will be dictated by the flight altitude and Mach number. If the vehicle deviates from the designed trajectory,

combustor temperature can reach the flow dissociation limit without compressing enough air at upper limit of the air-breathing corridor. At the lower limit of the air-breathing corridor structural and thermal limit loads will be encountered. Therefore altitude and Mach number along with the inlet pressure field distribution will be needed for the inlet geometry control.

Inlet shock attachment directly influences combustion efficiency. In the supercritical condition shown in Fig. 4.3.3 the forebody shock is outside the cowl lip. The effective mass capture area decreases and there is an increase in the total wave drag. In the subcritical condition, the bow shock is swallowed by the inlet, reflecting shocks inside the combustor will interfere with optimal combustion and may cause unstart. Therefore precise angle of attack and/or pitch angle measurement is needed to match the shock at the critical condition (Fig. 4.3.2) with the cowl lip. However, aerothermodynamic calculations of the interaction between the inlet shock and cowl lip indicate that shock impingement at the critical condition should be prevented because the heat transfer rate increases with shock impingement by an order of magnitude (according to the reference 9, about 20 times). Consequently the shock must be regulated so that the inlet stays just slightly in the supercritical condition as close as possible to the critical condition.

Another issue arises from the thickness of the boundary layer on the forebody. Due to the fuel dissociation in the boundary layer flow, that portion of mass flow in the hot boundary layer can not be used for producing thrust. In other words, thickening of the hot boundary layer results in decreasing thrust. Taken from an investigation of stratification in scramjet inlet flow by Lewis M.¹³, Fig. shows that as much as 50% of the inlet mass flow will be in the extremely hot boundary layer at the high Mach number and high altitude condition.

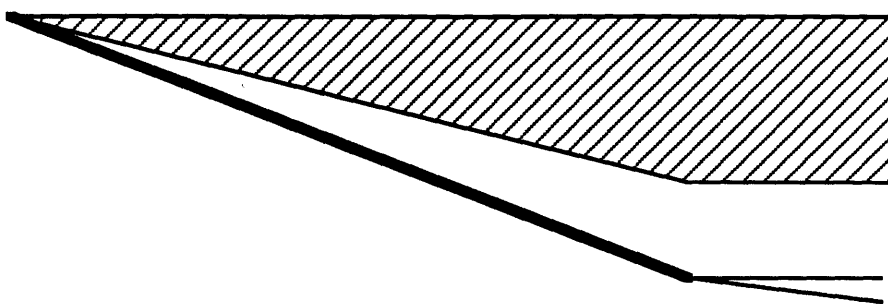


Fig. 4.3.2 Critical Operation

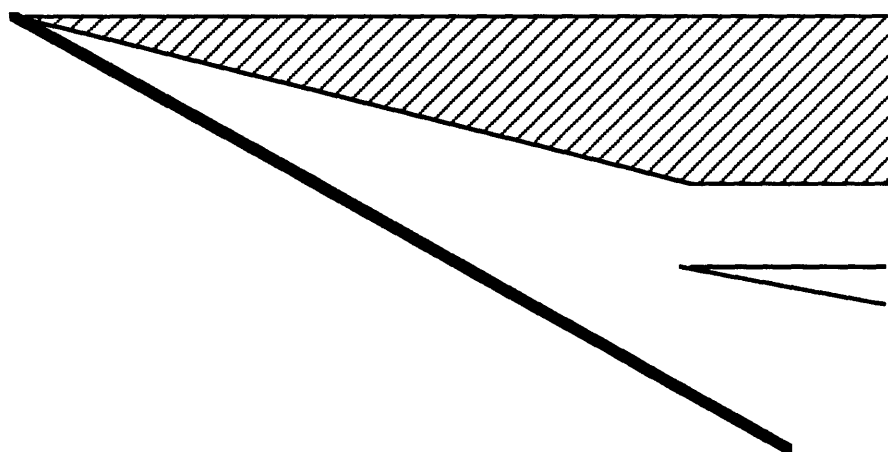


Fig. 4.3.3 Supercritical Operation

The boundary layer thickness is dictated by the vehicle attitude since the hypersonic boundary layer on the lower forebody will increase as angle of attack decreases. Boundary layer thickness is inversely proportional to forebody wedge angle and the angle of attack. Consequently increase in angle of attack will result in higher thrust within nominal design angle of attack range. Thus thrust and combustion processes can be modulated by vehicle short period oscillation (i.e. change in angle of attack). Due to the location of the air-breathing engine on the underside of the vehicle, pitching up moment would result as angle of attack increases. The thrust induced pitching moment will tend to cause instability and must be actively controlled.

The boundary layer thickness is also a function of altitude. As altitude increases, density decreases and as a result the boundary layer thickness increases. The altitude effect is quite large because kinematic viscosity increases nearly exponential in the atmosphere.¹³ In Fig. 4.3.4, 10% of thrust is expected to decrease at Mach number 20, altitude of about 120Kft, and dynamic pressure of 1 atmospheres.¹³

4.4 PROPULSION CONTROL SYSTEM

As described above, air data and inlet flow field parameter measurements are needed by the propulsion control system. The air data sensing requirements for the airbreathing hypersonic vehicle strongly depend on performance requirements of the scramjet. Due to absence of a flow mixing compressor, upstream flow conditions and vehicle motion will directly influence the combustion process. Beyond the guidance requirement to put the vehicle into a desired trajectory, the flight control and the air data systems must function as part of the propulsion control system.

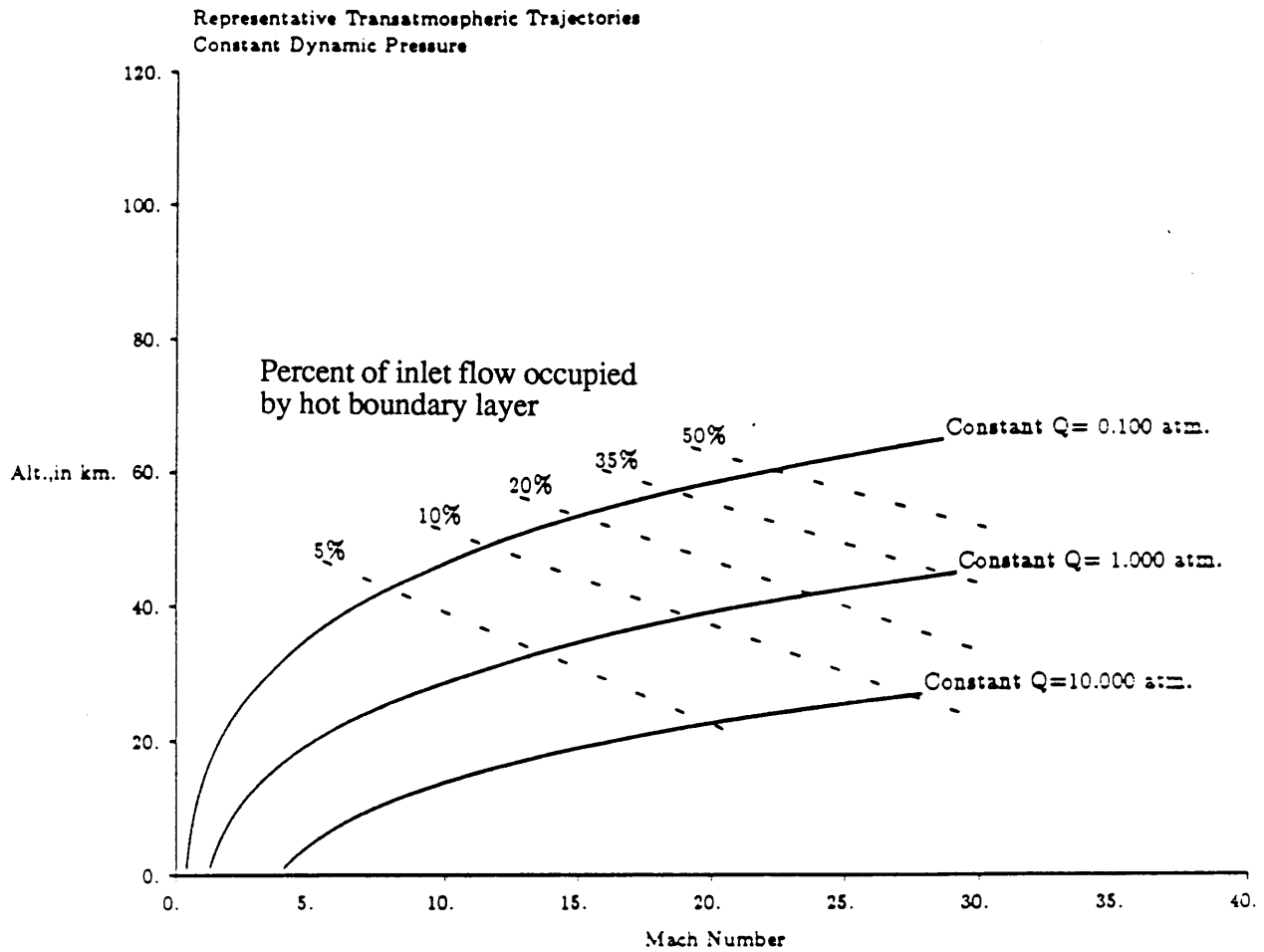


Fig 4.3.4 Percent of inlet flow occupied by boundary layer at 10 m wall cooled to 2000°K

taken from ref.13

One possible way of controlling the shocks and flow qualities inside the scramjet engine is to vary the inlet geometry as shown in Fig. 4.4.1. Since the shock angle is proportional to the body incidence angle for small angles, the shock angle can be efficiently controlled by the movable surfaces on the vehicle. By controlling the shock geometry of the inlet and the combustor, the combustor pressure and temperature can be regulated. Flow dumping bypass doors used in the SR-71 are not likely to be implemented, because the hot hypersonic boundary layer flow would likely destroy the bypass door mechanism. The implementation of a moving surface shock controller will be extremely difficult since it would require large actuator power. The power spectral density of the scramjet inlet flow disturbance is unknown, therefore the exact bandwidth requirement for the both sensor and the actuator is not available. In the variable geometry control, main limitation would be the actuator dynamics. The variable surfaces with hydraulic actuators would have maximum bandwidth of 10 to 100Hz. For the further analysis, 100Hz was picked as the target sensor bandwidth.

A general overview of a candidate scramjet propulsion control system is shown in Fig. 4.4.2. Since upstream flow condition and vehicle motion directly influence the desired inlet variables, upstream parameters are measured and the theoretical optimum control law for the whole engine could be determined. The measured upstream flow parameters and vehicle attitude information would therefore be fed into a central controller which would regulate the inner loop controllers.

The inner control loops consist of inlet, combustor, and nozzle regulators. For the inlet control, inlet geometry and cooling fluids would be controlled to provide an adequate combustion environment as well as regulate mass flow rate and to prevent material failure by active cooling. In addition, combustor information would feed back to the central controller to readjust the inlet variables. Inlet temperature, pressure, and shape would be

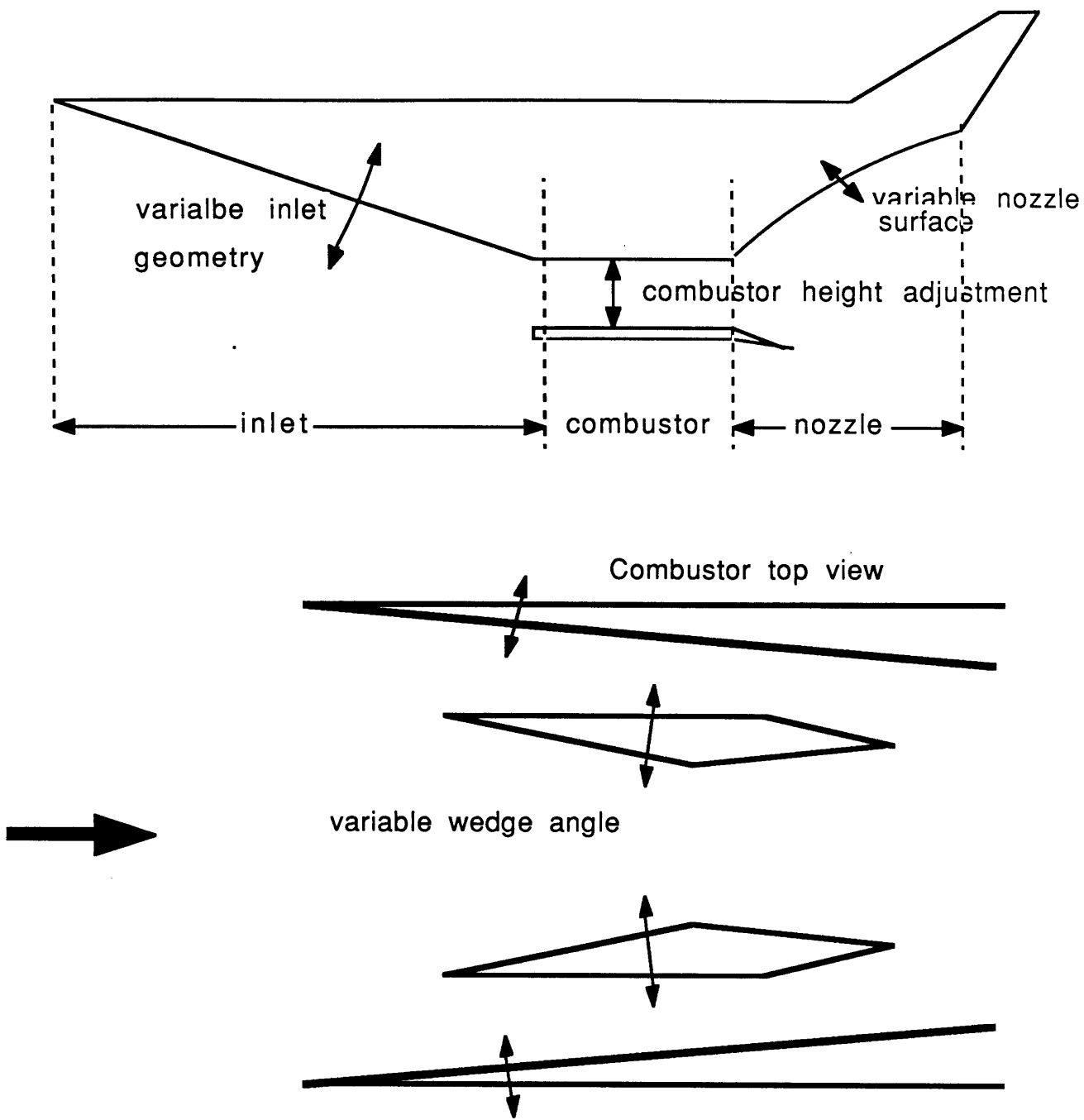


Fig. 4.4.1 Simplified Diagram of Vehicle Movable Surfaces

measured to predict inlet shock geometry, mass flow rate, and inlet flow field temperature and pressure.

In the combustor, fuel flow, coolant flow, and combustor height would be regulated based on the measured combustor temperature, pressure, and flow Mach number. In the nozzle, geometry would be regulated to provide adequate flow expansion. The combustor information would also be used to determine optimal nozzle shape.

In terms of outer loop of the control, the engine must provide good thrust command following to stay in the desired trajectory while regulating inner loop variables to prevent unstart. This predicted scramjet propulsion control system scheme suggests that the engine control could become very complicated since the vehicle motion, flow disturbance, and engine performance are highly coupled together. Consequently the air data system must provide quality flow information in order to control the coupled flight control and propulsion control systems. Also the air data system must be fault tolerant in order to be used as a part of the flight and propulsion control systems.

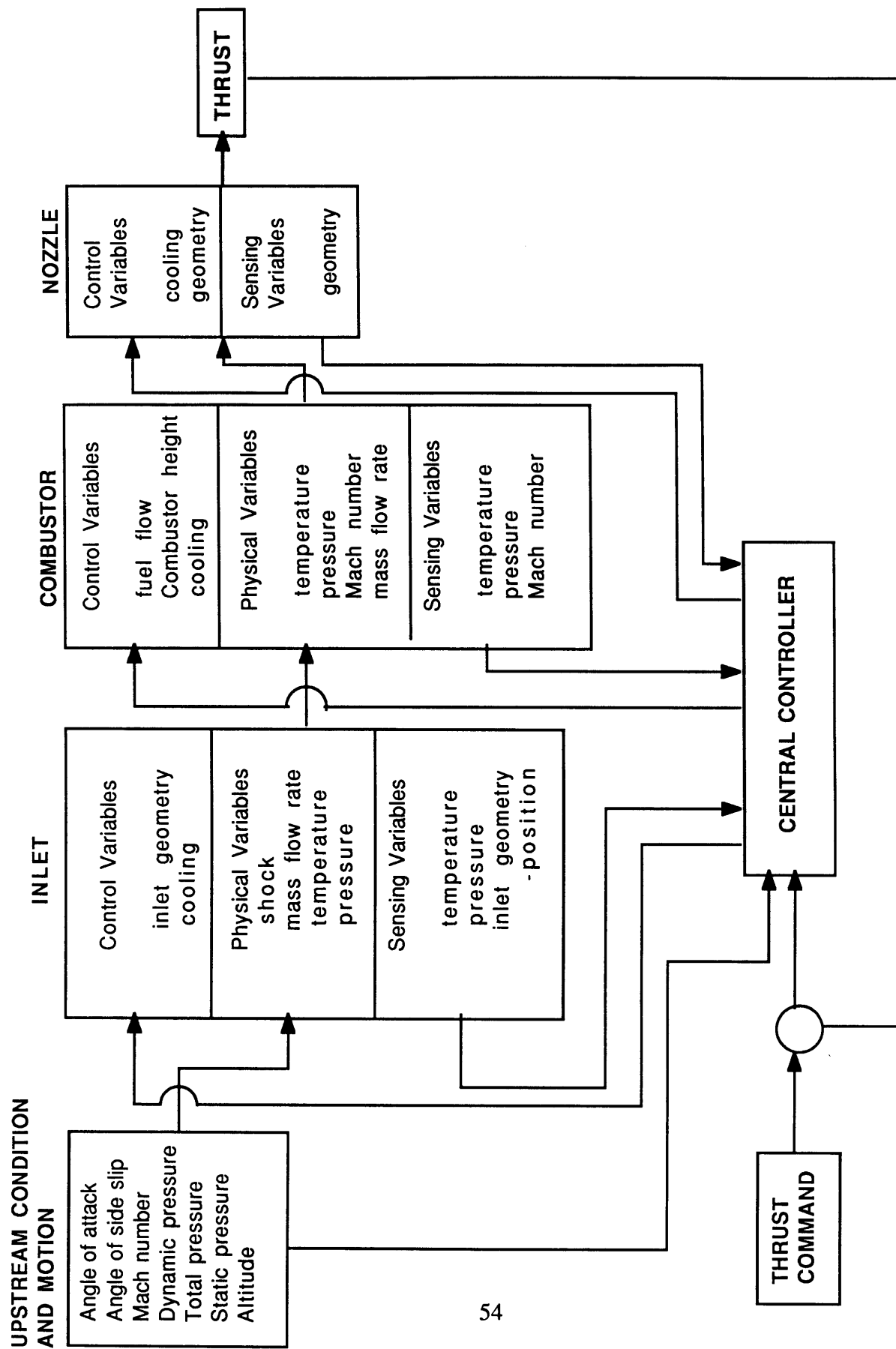


Fig. 4.4.2 Block diagram of Scramjet Propulsion Control System

5.0 PRELIMINARY AIR DATA MEASUREMENT SPECIFICATIONS

A preliminary set of the air data measurement specifications is discussed in this chapter. Table 4 summarizes the specifications for each parameter which will be discussed briefly below.

5.1 ANGLE OF ATTACK

The flow direction parameters such as angle of attack and angle of side slip are estimated to be critical parameters in scramjet performance. These parameters determine the shock geometry, combustor flow temperature and pressure distribution. Consequently the flow direction parameters will affect the scramjet engine performance. The angle of attack (α) accuracy is dictated by engine efficiency and inlet shock position considerations. The thrust coefficient, which is the thrust normalized by the dynamic pressure and inlet capture area, is a function of Mach number and angle of attack. Some information on the scramjet performance based on NASA Langley tests are available.¹⁷ In Fig. 5.1.1, the thrust coefficient is plotted with respect to the sum of the forebody wedge angle and the angle of attack. The thrust coefficient plot is available for Mach numbers of 5, 6, and 7. The scramjet engine is observed to be most efficient near the combustor choke condition. A 1° of change in angle of attack would result in about 5% thrust variation. When a realistic thrust to weight ratio of 1 to 2 is considered, the 5% thrust variation can be significant. For 1° control of angle of attack, a 0.1° accuracy in angle of attack measurement is considered desirable.

AIR DATA MEASUREMENT SPECIFICATIONS

		<u>Range</u>	<u>Accuracy</u>
Angle of Attack	α	5° from shock impingement	0.1°
Angle of Side Slide	β	$\pm 7^\circ$	0.1°
Mach Number	M	0-25	5-10%
Dynamic Pressure	q_∞	200 - 4300psf	5-10%
Total Pressure	P_t	1000 - 4300psf	
Static Pressure	P_∞	10 - 2100psf	0.3%
Altitude	h	0 - 150 K ft critical 150 K ft \Rightarrow orbital	5%
Vertical Velocity	\dot{h}	0-1000 ft/s	5%
Total Temperature	T_0	1200 -3000° F	
Inlet Pressure	P_{inlet}	1000 -4300psf	
Inlet Temperature	T_{inlet}	1200 -3000°F	

TABLE 4

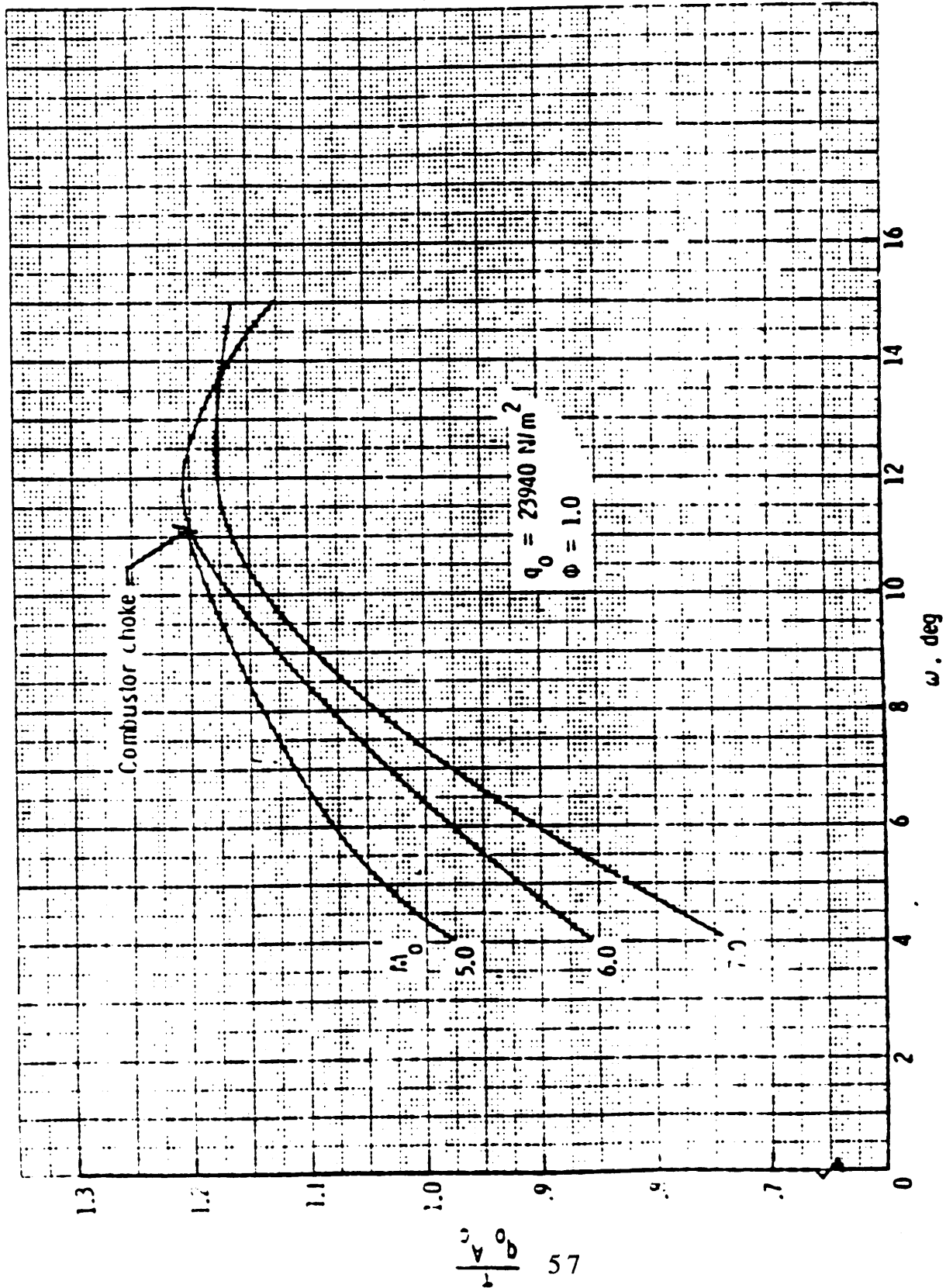


Fig 5.1.1 Thrust coefficient of Langley scramjet engine taken from ref. 17

A similar estimate of the required angle of attack accuracy can also be derived from the inlet shock attachment consideration. The combustion efficiency of airbreathing engines such as ramjet or scramjet depend on the shock positions in front of and inside the inlet. In order to optimize the engine efficiency, the compression shock must impinge on the cowl lip. Consequently airbreathing engines need to operate near the critical operation. For inlet shock control, over a 10 meter reference scale with 10 cm cowl lip thickness a 0.1° angle of attack accuracy is needed to prevent the shock detachment.

The maximum range of angle of attack during the hypersonic cruise would be no more than 5° based on the Langley test results.¹⁷ According to the thrust coefficient vs angle of attack plot in Fig. 5.1.1, 5° decrease in angle of attack would result in 30% reduction in thrust at Mach 7. The high sensitivity of scramjet engine with respect to the angle of attack can be explained by illustrating the changes in the thermodynamic parameters of the flow entering the combustor with respect to the changes in angle of attack. For the 5° wedge angle and 5° expansion angle forebody as shown in Fig. 5.1.2, the variation in inlet exit flow pressure and temperature with respect to the variation in angle of attack are computed by the 1-dimensional oblique shock relations. The results are plotted in Fig. 5.1.3 and Fig. 5.1.4. The inlet exit flow pressure and temperature changes substantially as angle of attack changes. As angle of attack changed 5° , both the flow pressure and temperature changed by a factor of two. Regulation of angle of attack within narrow operating range is critical.

5.2 SIDE SLIP ANGLE

The angle of side slip (β) accuracy requirements also result from inlet flow considerations. Recent CFD investigations on scramjet performance indicates that lateral

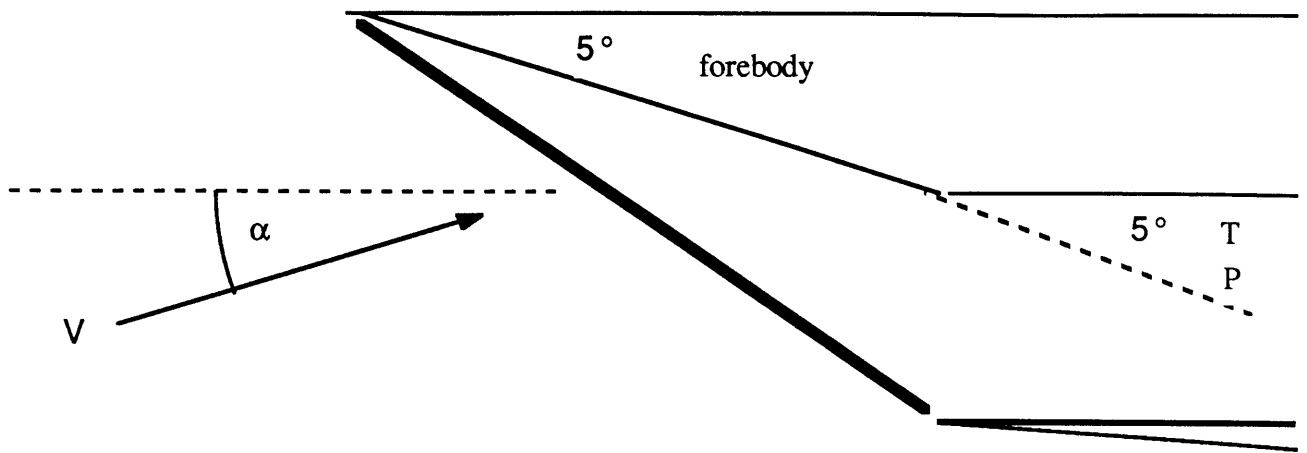


Fig. 5.1.2 5 degree wedge inlet model

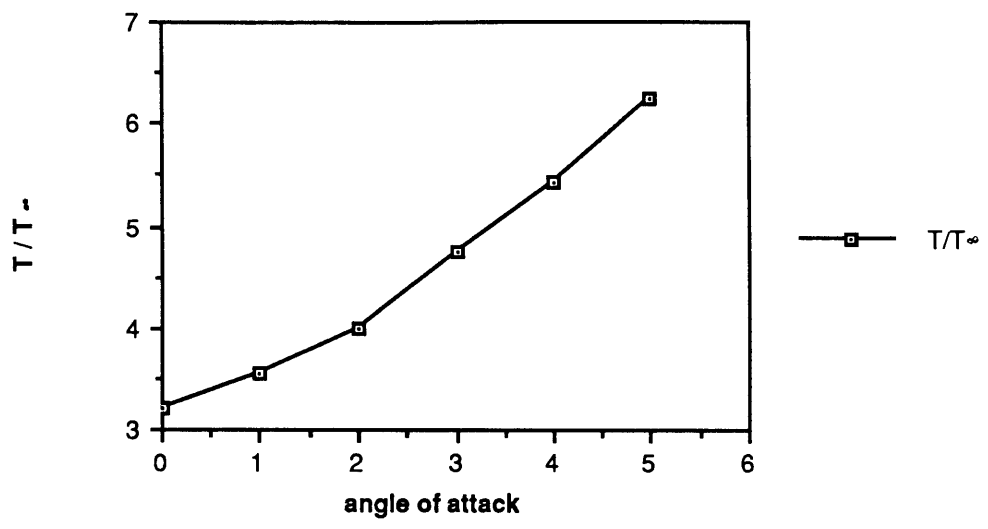


Fig. 5.1.3

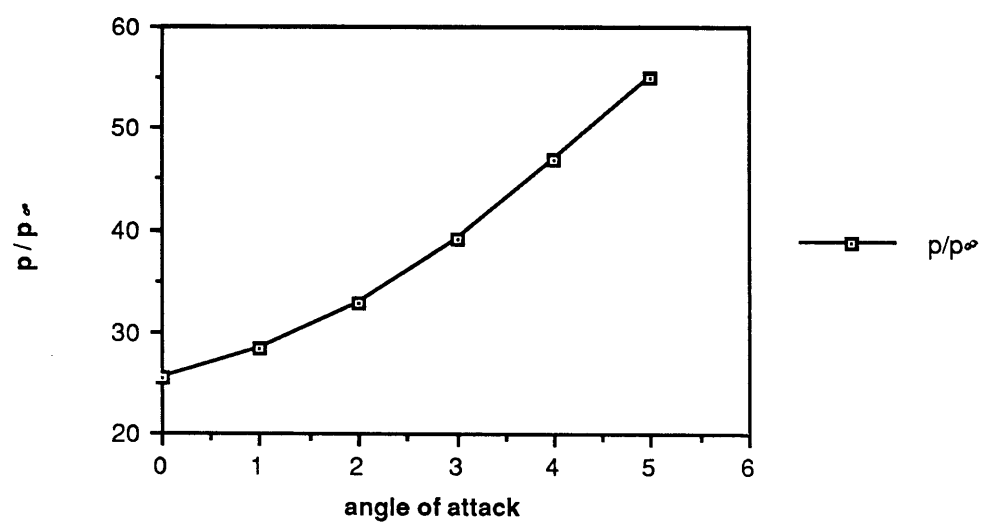


Fig. 5.1.4

inlet flow direction is also an important factor in the propulsion system performance.¹⁰ The scramjet flow direction sensitivity results were based on the NASA two strut design without combustion.¹⁰ An example of the solution of the Euler Equations for the engine is shown in Fig. 5.2.1 at a Mach number of 3 for 0° and 7° yaw angles. In the yawed condition, the pressure builds up in the inlet due to a strong bow shock and causes unstart. For the unyawed case the total pressure loss in the mid channel is about 26%. The total pressure loss increases to about 75% when unstart occurs. In Fig.5.2.2, yaw angles of 0° and 5° are compared at $M = 5$. The density contours suggest that the effect of asymmetry is very large. At a yaw angle of 5° , the shock induced by one of the side walls totally disappears and a strong asymmetry or distortion of the flow occurs. Even though the flow did not unstart the engine, the shock geometry, density and pressure distribution is altered. The degree of combustor sensitivity with respect to the gas states and flow field inside the combustor is difficult to determine due to lack of understanding in high speed combustion. However from this comparison, it's clear that small changes in the flow direction can alter the combustion state and move the engine off the optimal operating point. The specific accuracy requirement on the side slip angle(β) measurement is unknown due to lack of information on the scramjet sensitivity with respect to the side slip angle. However, more precise regulation of side slip would result in more efficient engine operation so a value similar to the α value of 0.1° was indicated in Table 4.

5.3 MACH NUMBER

The ramjet would likely operate Mach number 2 to 6 and scramjet would take over from Mach 6 to the combustion limit of between Mach 12 and 25. Consequently, the flight Mach number measurement is not considered to be critical other than for guidance purpose. An estimated accuracy of 5-10% for Mach number will be adequate for such purpose.

Even though the flight Mach number measurement is not critical, the Mach number measurement is extremely difficult at $M > 4$. Mach number is usually obtained by the Rayleigh pitot formula which is;⁴

$$\frac{q}{p} = \frac{1 + \gamma}{2} M^2 \left[\frac{(1 + \gamma)^2 M^2}{4\gamma M^2 - 2(\gamma - 1)} \right]^{\frac{1}{\gamma - 1}} - 1$$

and the dynamic pressure relation can be written as

$$q = \frac{\gamma}{2} M^2 p$$

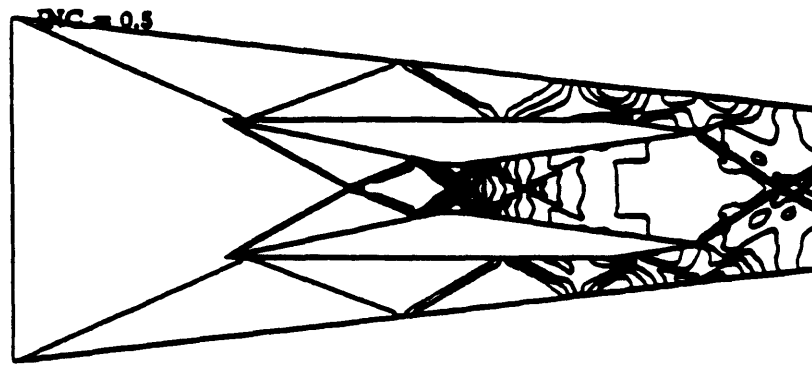
For Mach number greater than 1 and $\gamma = 1.4$, the above equations become

$$q = \frac{1}{1.84} \left[1 - \frac{1}{7M^2} \right]^{2.5} p$$

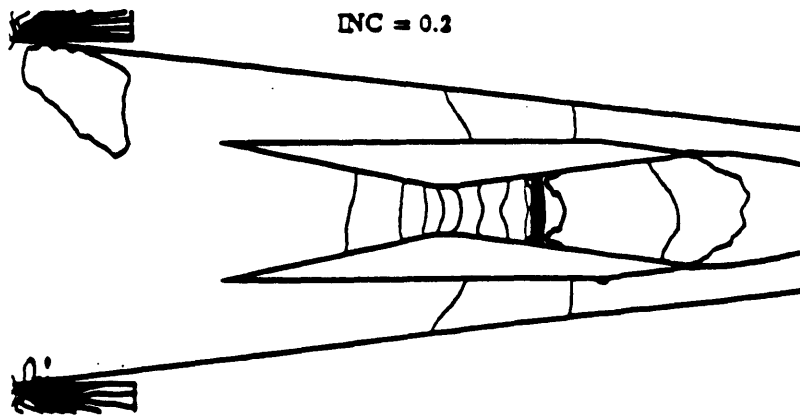
Therefore at high Mach numbers q/p approaches to 0.54. Due to very little variation of the dynamic pressure and total pressure ratio, Mach number measurement become very difficult.

5.4 DYNAMIC PRESSURE

Dynamic pressure measurement is required by the propulsion system to maintain the inlet pressure between 1/2 to 2 atmospheres (1100 to 4400 psf). Also, aerodynamic loads and thermal loads are related to the dynamic pressure. The estimated maximum dynamic pressure is 2 atmospheres due to the structural limitations. Dynamic pressure is typically inferred from measurements of total pressure, static pressure and Mach number. If active control is implemented to regulate the inlet pressure, the dynamic pressure measurement accuracy requirement would be similar to the case of the Shuttle or the X-15.



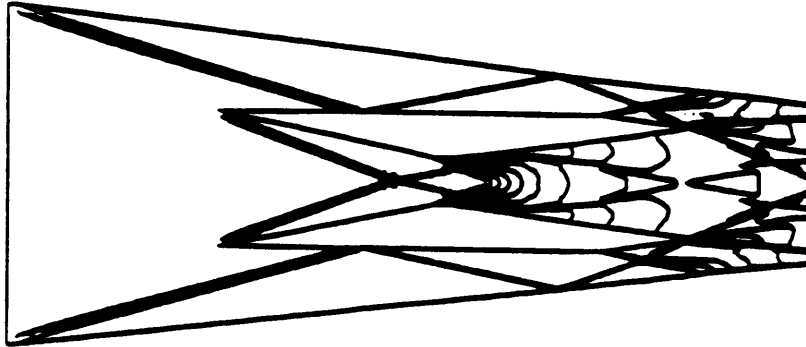
Pressure, $M_{\infty} = 3$, $\alpha = 0^\circ$



Mach Number, $M_{\infty} = 3$, $\alpha = 7^\circ$

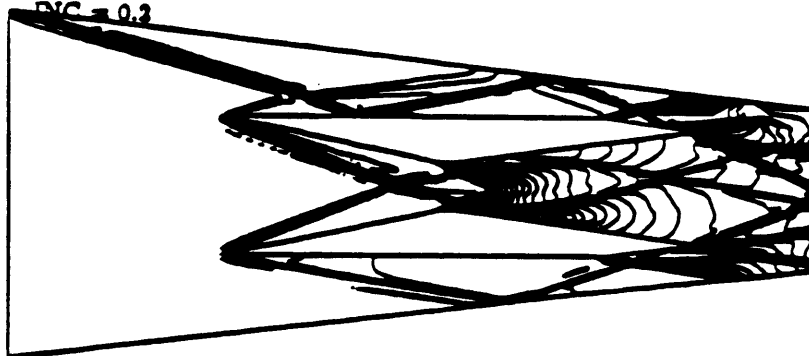
Fig 5.2.1 Pressure contour of Scramjet at $M=3$ taken from ref.10

INC = 0.5



Density, $M_{\infty} = 5$, $\alpha = 0^\circ$

INC = 0.3



Density, $M_{\infty} = 5$, $\alpha = 5^\circ$

Fig 5.2.2

Density contour of Scramjet at M=5

taken from ref.10

The estimated accuracy requirement of 5% is proposed. At high Mach numbers, dynamic pressure become primarily a function of stagnation pressure and Mach numbers. The dynamic pressure equation become;⁴

$$Q = \frac{\gamma}{\gamma + 1} \left[\frac{4\gamma}{(\gamma + 1)^2} - \frac{2(\gamma - 1)}{(\gamma + 1)^2 M^2} \right]^{\frac{1}{\gamma - 1}} P_t$$

The dynamic pressure measurement accuracy will improve as Mach number increases since errors in static pressure measurement do not contribute and Mach number contribution decreases significantly. However, as the surface temperature increases, real gas effect should be considered. The specific heat γ will decrease as the gas temperature increases. Correction of the specific heat for real gas effects may be needed.

5.5 STATIC PRESSURE AND ALTITUDE

The static pressure is one of the most difficult parameters to measure. Position error, which results from imperfect static port location, contributes significantly to uncertainty in the static pressure measurement. Altitude can be measured by either the radar altimetry or by static pressure measurement. If pressure altimetry is used, then the accuracy requirement on static pressure would be 0.3% of sea level pressure based on a 5% altitude precision at 100,000 ft. If the static pressure measurement is only used for calculating dynamic pressure a 5% uncertainty is thought to be acceptable.

5.6 INLET PRESSURE

To provide a good combusting environment at the combustor, the flow quality of air in the inlet exit are needed. For the estimation of the combustor states, several inlet

pressure measurements are needed. The optimal range for the inlet pressure is between 0.5 to 2 atmospheres. Higher compression (i.e. increase in inlet pressure) means higher engine performance, but structure may not withstand such high pressure and temperature. The engine may be able to operate at 0.1 atmosphere but far less efficient than the optimal range. The inlet pressure measurement accuracy specification can not be defined due to lack of the scramjet engine control model. If the vehicle rely on the ramjet or dual combustion scramjet during part of the flight, the inlet pressure measurement accuracy requirement would be similar to the SR-71, which is the 0.1%.

5.7 INLET TEMPERATURE

Ideally inlet temperature should be near 1200°F where the combustor flow temperature is hot enough to provide spontaneous combustion and cold enough to add energy. The stagnation temperature which may be as high as 3000° F is needed to estimate the combustor temperature. Actual specifications will depend on the engine performance data which is unavailable at this time . Generally, higher precision will allow more efficient fuel air mixture control and higher combustion efficiency.

5.8 SHOCK LOCATION

The angle of the oblique shock in front of the forebody and the oblique shock geometry inside the combustor are desirable to measure. The initial oblique shock determines the engine inlet efficiency and the oblique shock geometry inside the combustor determine the pressure and temperature field inside the combustor. In principle, the shock angle can be obtained by the inlet wedge surface pressure measurement with other air data parameters such as Mach number, static pressure, and the free stream flow direction. However, actual implementation is difficult, because, the Mach number measurement is

very difficult above $M > 4$ and the static pressure measurement is difficult. The optical techniques, which are described in next chapter, may be the better candidate for the shock angle measurements.

6.0 AIR DATA SENSING TECHNIQUES

Air data sensor systems for hypersonic vehicles require non-intrusive, reliable, high bandwidth (in the order of 100Hz) performance. There are several non-intrusive air data sensing concepts available. Most feasible concepts are pressure measurement techniques and optical techniques. These concepts are briefly described below:

1) **Surface Pressure Measurement Technique:** The air data parameters such as the flow direction parameters (α, β), altitude, etc, have a direct relationship with the vehicle surface pressure distributions. By having a either empirical and/or analytical relationship of the vehicle surface pressure with respect to the air data parameters, the pressure sensor system can be installed flush to the surface and avoid the intrusive pitot-static probe. More detailed information is discussed in next section.

2) **Ultra Violet (UV) densitometer:** The UV densitometer concept was proposed for the X-20A in the early 60's to measure the flow near the bow shock of the entry vehicle.¹⁵ The UV beam would be transmitted through the window located on top of the vehicle. Due to the density variation of the flow, transmitted UV beam is scattered and reflected back to the UV receiver located on the fuselage, behind the transmitter.

3) **E-beam air data sensor:** Similar to the UV densitometer, E-beam air data sensor is based on scattered UV light detection.¹⁵ An electron beam is produced by an electron gun located inside the fuselage and the beam would be emitted to the atmosphere through the fuselage window. The electron beam is scattered by the external flow and excites the air and emit ultra violet light. Photo multiplier tube, which located down stream, pick up the UV light scattering. The electron beam sweeps through the flow region of interest and detect the external flow condition in various region

4) **Laser Doppler Velocimeter:** The flow velocity can be measured by detecting the Doppler frequency shift of laser light that has been scattered by particles inside the flow. Usually two laser beams are emitted to the atmosphere through the window and crossed to produce interference pattern. When the sub-particles in the external air flow pass through the crossed beam region, light is scattered and Doppler shifted due to the particle velocity. A photo-detector is used to detect the scattered light and extract the particle velocity from the Doppler shift. The flow velocity can be inferred from the assumption of the particle velocity is equal to the flow velocity.

5) **Laser Holography:** The laser holography can be used to detect the flow field density variation. There are some cases (Langley Hypersonic Wind-Tunnel Tests) that the laser holography technique is used on high speed wind-tunnel tests instead of the Schieren method. The density variation in the flow field such as shock structures result in refractive index changes of the coherent laser beam. Refractive index changes imposes phase shifts on an optical wave that can be observed in the fringe variations of an interferogram. By interpreting the fringe variations, the flow field description can be obtained.

All of the above techniques, in principle, can be used to measure the external flow field without protruding probes. However several of these techniques are not readily applicable for the hypersonic air data and propulsion state measurement sensors. Laser, E-beam, and UV based sensors require very complicated optical and electrical equipments, and they are far less reliable than pressure measurement concept. The optical techniques are hard to implement redundantly and therefore provide fault tolerance in the system. The optical techniques also require windows which would be difficult to place on the hot fuselage. Weight, volume, and power consumption would likely be much greater than a pressure sensor system with cooling. Therefore the surface pressure measurement

techniques is considered to be most viable technique for the hypersonic air data system if the required accuracy can be achieved.

6.1 FOREBODY SURFACE PRESSURE MEASUREMENT

Many of the required air data parameters can be inferred from surface pressure measurements around the forebody or nose of the vehicle in a manner similar to the Shuttle Entry Air Data System (SEADS). Unlike a pitot boom sensor, a flush orifice concept uses the fuselage (usually the forebody) as a pitot probe. Instead of eliminating the flow disturbances caused by the fuselage, the flush pressure sensors measure the pressure distribution of the forebody, then extract the fuselage contribution in order to obtain the air data parameters. The surface pressure field on the forebody can be measured by an array of the surface pressure sensors. By having a calibrated relationship between the pressure field and the desired air data parameters, the air data parameters can be extracted from the surface pressure field measurement. Some engine control parameters can be inferred from the surface pressure measurement in and around the inlet. Total temperature and inlet temperature would be measured separately.

The pressure measurement accuracy requirements can be obtained from the air data measurement specifications from Chapter 5. If the SEADS like scheme is used, then the air data system algorithm can be inverted to achieve the pressure sensor precision requirements. For example, the flow direction parameters (α, β) are related to the nose surface pressure as;

$$C_p = \frac{P_\theta - P_\infty}{q_\infty} = C_{pmax} \sin^2 \theta \quad \text{for } M \gg 1 \text{ (from modified Newtonian)}$$

where the θ is defined in Fig.6.1.1. The pressure coefficient at the pressure orifice 1 and 2 are;

$$C_{p1} = C_{pmax}(1 - \sin(\phi + \alpha))$$

$$C_{p2} = C_{pmax}(1 - \sin(\phi - \alpha))$$

then the difference ($C_{p1} - C_{p2}$) become;

$$\Delta C_p = -C_{pmax}\sin(2\phi)\sin(2\alpha)$$

The maximum sensitivity occurs at $\phi = 45^\circ$. By applying above equation with 0.1° angle of attack, the pressure transducer has to have accuracy of 0.3% of the stagnation pressure.

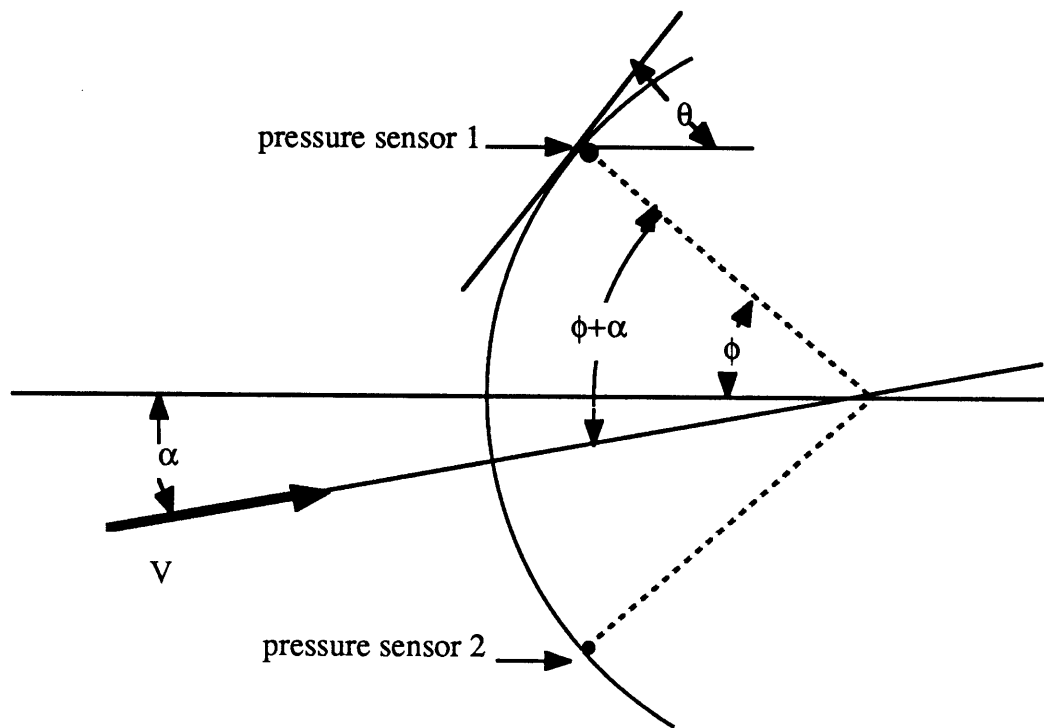


Fig. 6.1.1

6.1.1 FLOW MODELING

The accuracy of air data parameter estimation depends on the pressure sensor accuracy and the flow modeling accuracy. Computation of the functional relationship between the surface pressure and the air data parameters based on the complete vehicle model is very difficult. Moreover, providing air data parameters by such time consuming computation in real time would not be practical. Therefore simple approximated flow model is highly desirable.

The high velocity flow can be modeled by a modified Newtonian approximation of hypersonic flow which predicts the pressure field of a blunt body extremely well at relatively high Mach numbers. The advantage of modified Newtonian flow approach is in simplicity. The pressure coefficients around the body are simply a function of the pressure coefficient at the stagnation point and the body shape. The accuracy of the Newtonian approximation is most accurate at High Mach number and decreases with Mach number.

In the subsonic region, the solution of the pressure field can be obtained by the potential flow theory. The incompressible flow over spheroid can be calculated for the low speed flow. However, for Mach numbers over 0.3, compressibility can not be neglected. From high subsonic to supersonic flow, there are no simple mathematical approximations which exist to reconcile the inaccurate Mach number region of modified Newtonian and potential flow theory.

6.1.2 NUMERICAL TECHNIQUES

Estimation theory can be implemented to transform the pressure signals into air data parameters while minimizing error variance estimate of the air data parameters in the

presence of noise. The digital filtering technique which was implemented on the SEADS is extremely practical.¹ One of the advantages of such digital filtering is its inherent redundancy. Since there are multiple sensors (usually more sensors than air data parameters) the pressure measurements can be made even when some sensors fail. The primary disadvantage of this estimation technique was the relatively long processing time. If the air data application requires high bandwidth, the sensor filter technique may not be applicable.

6.2 PROPULSION STATE SENSING TECHNIQUES

In order to perform the difficult task of inlet control, the observability of the engine state, or inlet combustor flow state is important. The static pressure after the shock can be measured to detect the shock location and shock angle. Also the pressure measurement can be used to estimate the total pressure recovery with the detected shock geometry. The engine performance is directly related to the total pressure recovery.

Dynamic pressure measurement can be used by the scramjet to operate within the suggested airbreathing engine boundaries. Again, pressure measurement is needed as part of the control loop to regulate the variable inlet geometry. The shock position and angle can be estimated from pressure measurement on an array around the inlet lip. Differential pressure sensors can be mounted on the side of the inlet to detect inlet disturbances related to side slip and to predict the combustor state. In addition, the compression can be measured by placing the sensors on the underbody. Because of the control of shock geometry within the inlet will involve high bandwidth actuation, the inlet pressure sensor systems must therefore be high bandwidth and are required to be placed close to the surface. In this case active cooling of the sensors would probably be needed. It is possible

that at high Mach numbers the active inlet control scheme can not be implemented due to actuator weight and heating considerations. In that event, the shock geometry in a fixed inlet could, in principle, be controlled by flying an extremely precise (0.1°) angle of attack and side slip profile.

7.0 PRESSURE MEASUREMENT TECHNIQUES

In this chapter, the pressure sensor implementation issue will be discussed. The sensor system can be divided into the pressure orifice and transducer. Functional requirements for each of the components are discussed based on the hypersonic application constraints.

7.1 PRESSURE SENSING ORIFICE CONSIDERATIONS

The local surface pressure is defined as the normal force per unit area on the local region of the surface; therefore, the most direct surface pressure measurement technique is a method of mounting a transducer on the vehicle surface where the transducer diaphragm is a part of the vehicle surface as shown in Fig 7.1.1. Such a technique is not readily applicable in a hypersonic vehicle because the transducer would be exposed to high external heat loads. Most transducers could not handle the temperatures up to 3000°F which are expected during the hypersonic cruise. Also, the exposed sensors could be easily damaged by erosion. Therefore, the transducers will be isolated by a pneumatic tube. Commonly a hole is drilled normal to the surface and a circular pneumatic tube is installed to connect the hole and the pressure transducer as shown in Fig. 7.1.2. However there are problems associated with the pneumatic tube and transducer sensor system. The system has inherent absolute measurement error due to the flow disturbance caused by the sharp changes in surface boundary at the orifice. The sensor system is also bandwidth limited by the pneumatic tube addition to the bandwidth limit of the transducer. These bandwidth limitations are due to the pressure lag and acoustic resonance. More detail on the sources of error of the sensor system are discussed in next section.

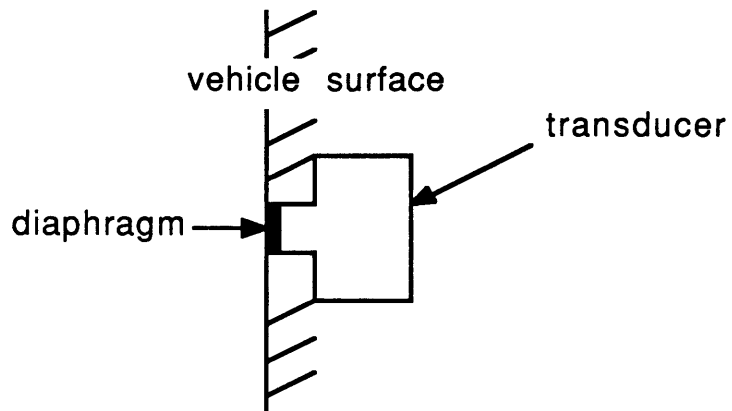


Fig. 7.1.1

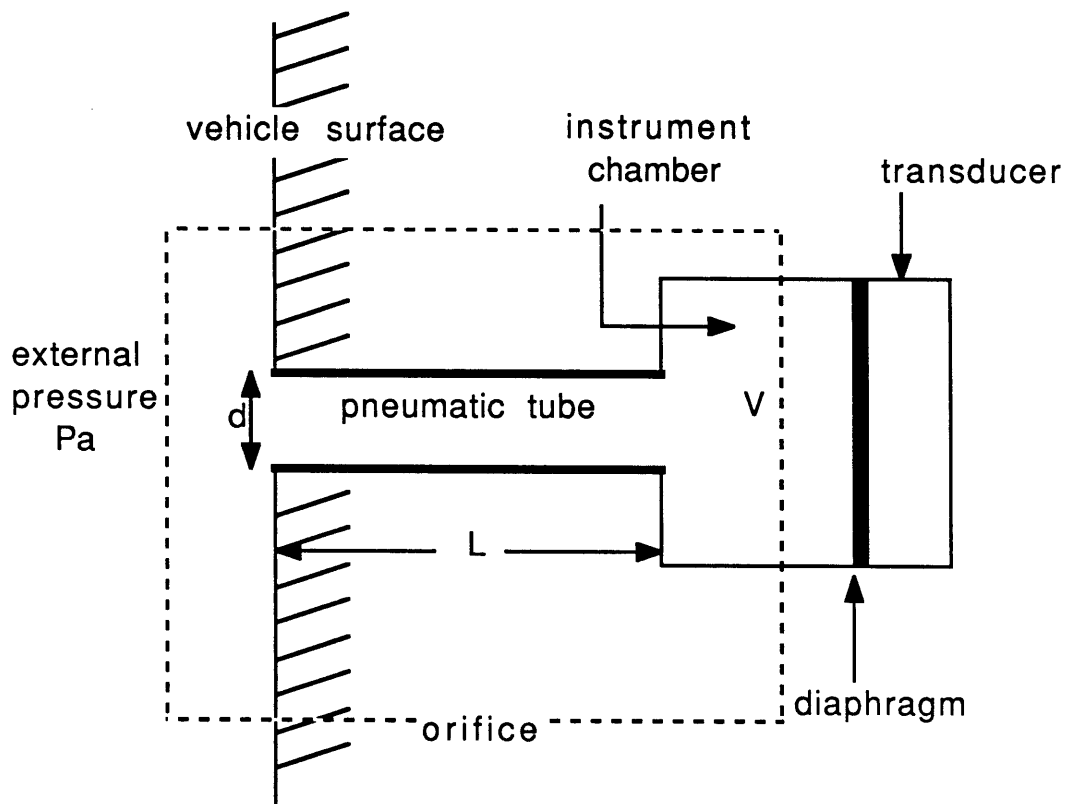


Fig 7.1.2

7.1.1 SOURCES OF ERROR

Pressure Lag: One of the bandwidth limiting factors in implementing a long pneumatic tube between the vehicle surface orifice opening and a transducer is pressure lag error. The pressure lag error is caused by the fact that the finite mass inside the tube has to flow into and out of the tube with frictional resistance in order to equilibrate the pressure difference. The finite time is required to equilibrate the pressure difference between the vehicle surface and the transducer. The dynamics of the pressure lag is analogous to a low pass filter. Steady state and low frequency fluctuation of the external pressure can propagate to the transducer, but high frequency pressure transients will be attenuated. For the simple cylindrical tubing with instrument chamber shown in Fig. 7.1.2, the pressure lag time constant is defined as below.¹⁸

$$\tau_{\text{lag}} = \frac{128 \mu L V}{\pi d^4 P_a}$$

The pressure lag time constant is a function of the external pressure, tube diameter, instrument chamber capacity, and tube length. The pressure lag will increase as the temperature of gas, which displaces the pneumatic tube, increases. The temperature effect is due to the air viscosity changes. In Fig. 7.1.3, the pressure lag time constant vs external pressure is plotted for air temperature of 1800°F, and 0.125 inch tube diameter, and LC (tube length, chamber capacity product) of 1 inch⁴. If the ambient pressure decreases due to the increase in altitude then the pressure lag will increase. In Fig. 7.1.4, the pressure lag time constant is plotted against both the tube length and the tube diameter for air temperature of 1800°F, external pressure of 1000 PSF. In the Fig. 7.1.4, the instrument chamber was assumed to be small. If the orifice tube length increases, then the

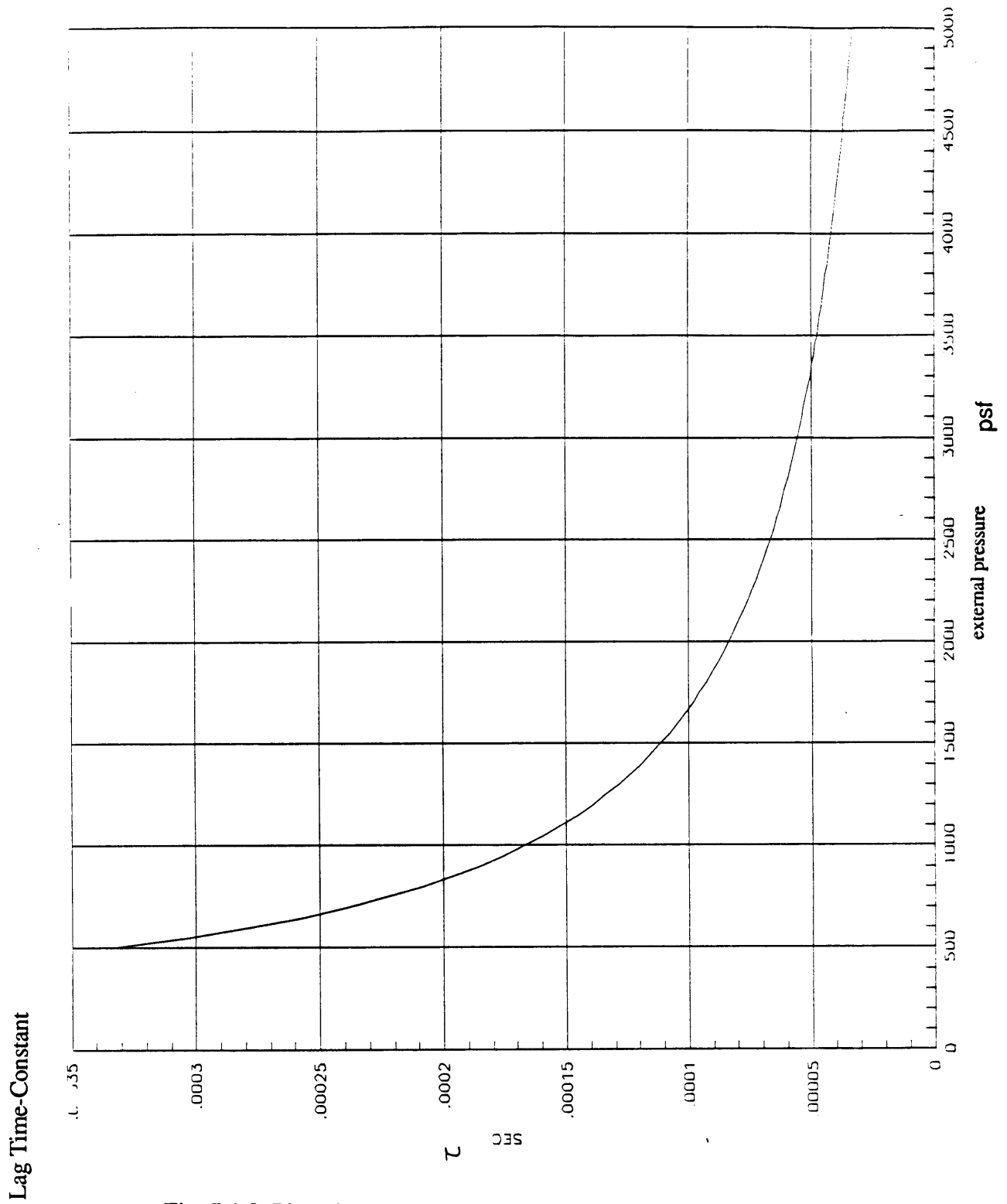


Fig. 7.1.3 Plot of Pressure Lag Time-Constant vs External Pressure

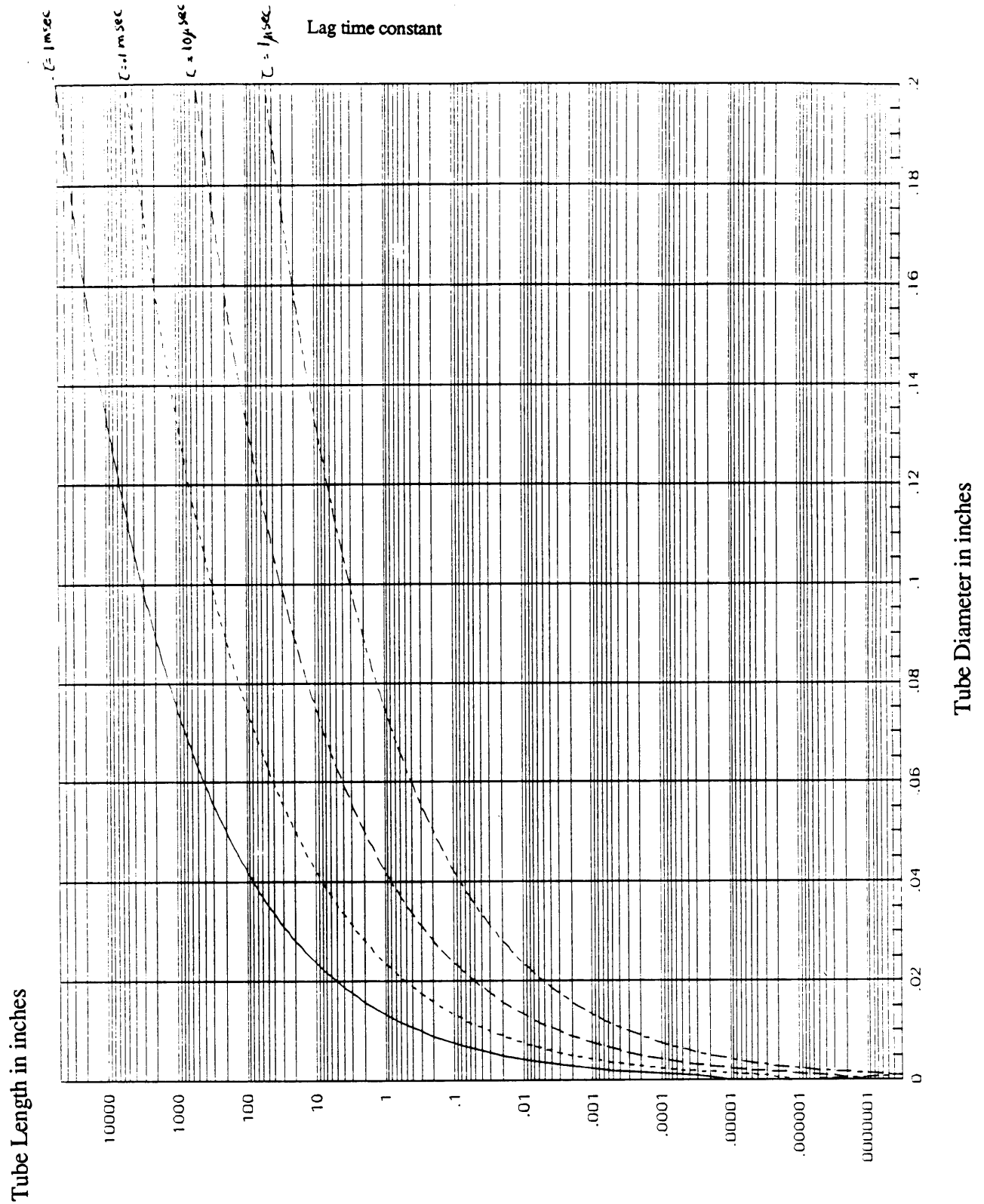


Fig. 7.1.4 Plot of Pressure Lag Time-Constant vs Tube Length and Diameter

pressure lag increases. Also, if the tube diameter decreases, then the pressure lag increases.

Acoustic Resonance: Whenever a transmission tube is used as shown in Fig. , the resonance will occur when the frequency of the pressure signal is tuned to an acoustic resonance of the system. The resonance will occur at the fundamental resonant frequency and its upper harmonics as shown in Fig. 7.1.5. The effective bandwidth of the orifice system is therefore limited by the fundamental resonant frequency. The resonant frequency must be far above the system bandwidth, otherwise the measurement error will result due to large amplitude changes in the region of the resonant frequency. The orifice system can be modeled as the Helmholtz resonator and the resonant frequency is defined as;¹²

$$f = \frac{c}{2\pi} \sqrt{\frac{a}{V \left(L + \frac{1}{2} \sqrt{\pi a} \right)}} \quad \text{where } a = 0.25\pi d^2$$

The bandwidth of the orifice rapidly decreases as tube length increases. The bandwidth decreases as the instrument chamber volume increases.

Orifice flow Error: Whenever surface pressure is measured with a sharp-edged, circular, static pressure hole normal to the boundary of the air flow, an error in absolute pressure measurement results due to the interaction between the flow and the sharp edge of the orifice. Large errors can occur if the hole has irregular rounded edges or any other surface distortions. Even if the orifice geometry is perfect, some residual error exist due to sharp changes in surface boundary and the flow disturbance occurs at that region. The error is a function of Reynold's number with respect to the hole diameter.²⁰ The error increases as the Reynold's number increases (i.e. also hole diameter increases).

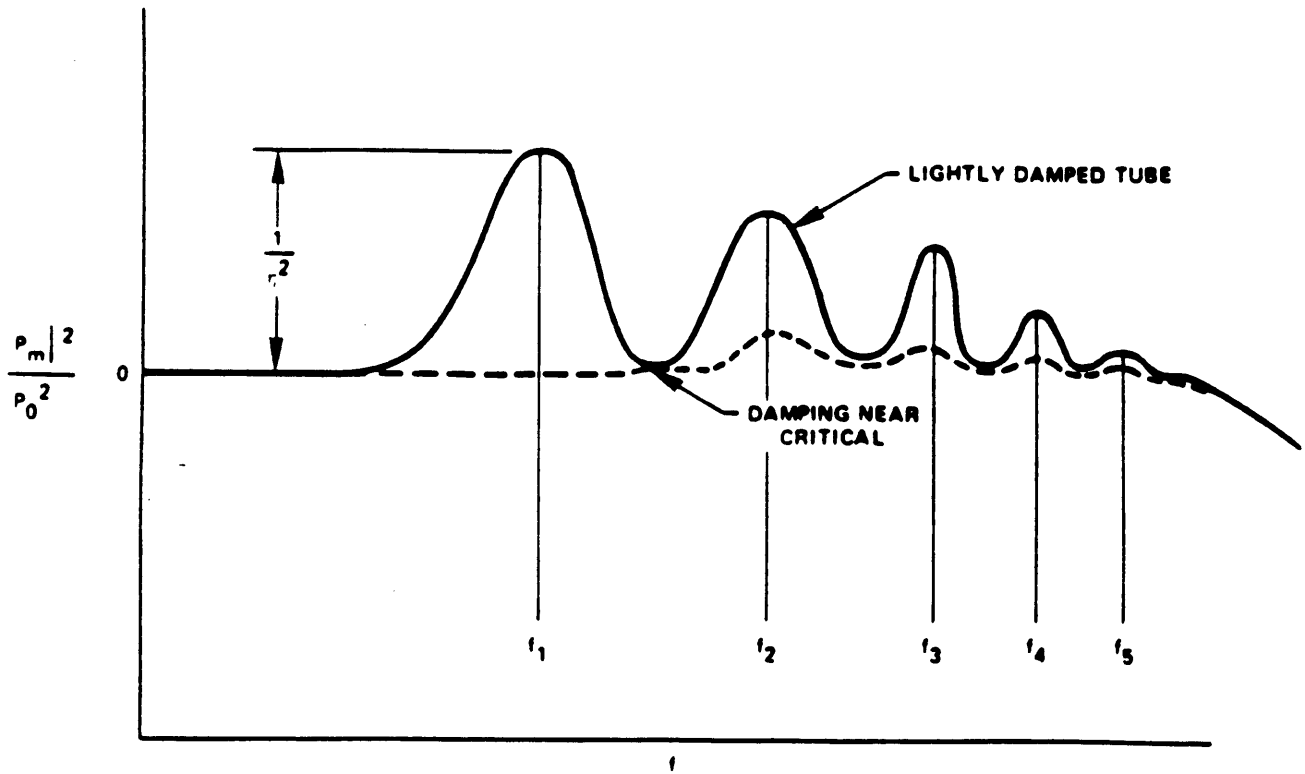


Fig. 7.1.5 Typical pressure response of pneumatic tube taken from ref. 12

P_m = pressure at transducer diaphragm
 P_o = pressure at surface

Temperature Induced Pressure Error: If the transducer is closely coupled to the surface with relatively large orifice diameter, convection can occur inside the pneumatic tube due to large temperature gradient between the transducer and the vehicle surface. The convection inside the orifice will cause flow disturbance and results in pressure measurement error.

Position Error: Position error is the static pressure measurement error which is dependent on the position of the static pressure orifice. Normally the static pressure orifice location is selected on the fuselage (usually on the side of the fuselage) so the static pressure measurement error is stationary in the presence of attitude and Mach number variations. Even though the best location is selected on the fuselage, a difference between true static pressure and measured static pressure exists due to the fact that the fuselage disturbs the flow. Position error can be calibrated by the empirically derived error correction factor from wind tunnel or inflight tests.

8.0 SENSOR SYSTEM THERMAL CONSIDERATIONS

The sensor thermal problem is considered in this chapter. Thermal considerations are critical for transducer selection and orifice design. The surface peak temperature will be determined by the vehicle flight trajectory. The integrated heat load on the vehicle are determined by the flight trajectory, cruise duration, and vehicle thermal insulation and/or cooling technology. Once the flight trajectory and duration are determined, sensor thermal designs can be evaluated. A heat transfer model of the orifice is constructed to aid in evaluation of the transducer thermal requirements. The model is based on a simple pneumatic tube and instrument chamber configuration as shown in Fig. 8.0.1.

In Fig. 8.0.1, the primary potential heat flow routes are shown. Heat can be transferred through the vehicle surface, there by heating up the pneumatic tube and the vehicle's internal air. Heat can be transferred to the transducer by three routes; through the air column, through the pneumatic tube walls, or through the heated internal structure.

Radiative Heat Transfer: Thermal energy can be emitted by a heated body through electro-magnetic radiation. If the heat-radiating body can be assumed to be an ideal radiator (i.e. black body), then the thermal energy emission will be proportional to the fourth power of the absolute temperature. The thermal exchange between two ideal radiators can be described as;¹⁹

$$q = \sigma A (T_1^4 - T_2^4)$$

where σ is the Stefan-Boltzmann constant and T_1 and T_2 are the temperatures of two black bodies. The radiative heat transfer from a hypersonic vehicle surface would be very large.

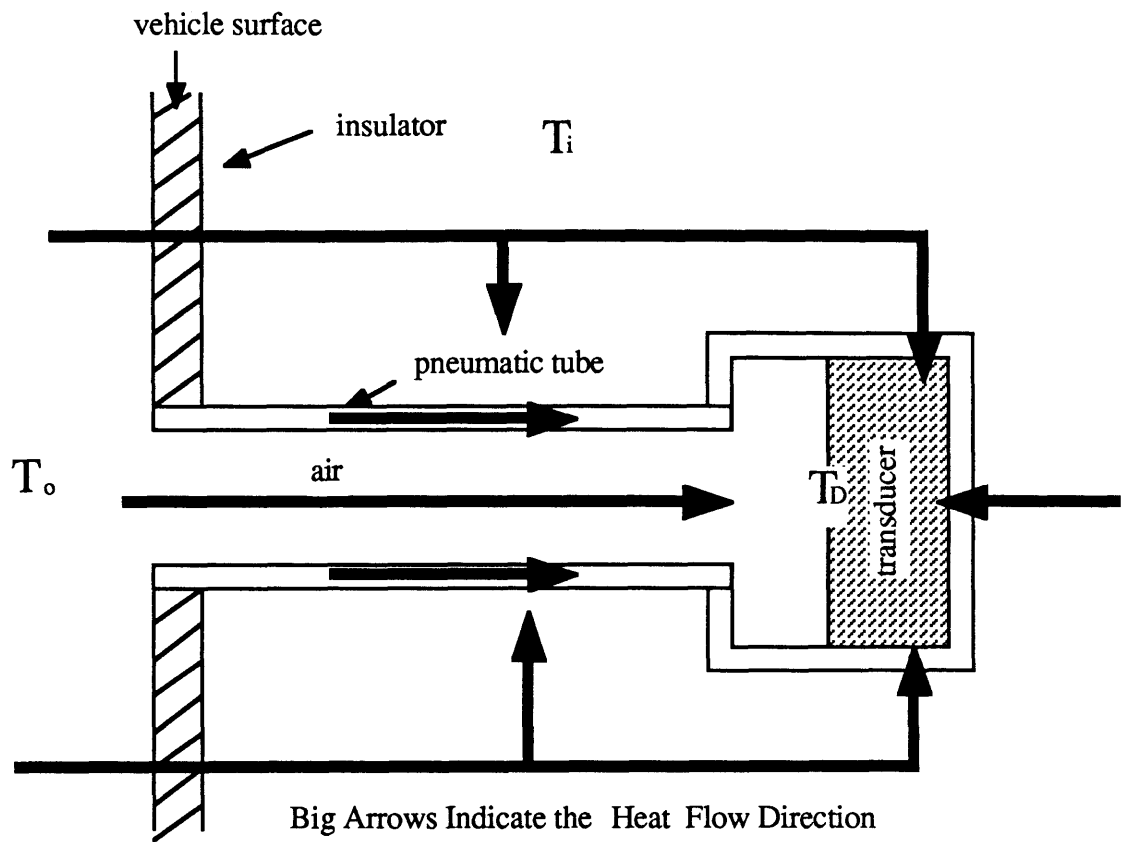


Fig. 8.0.1

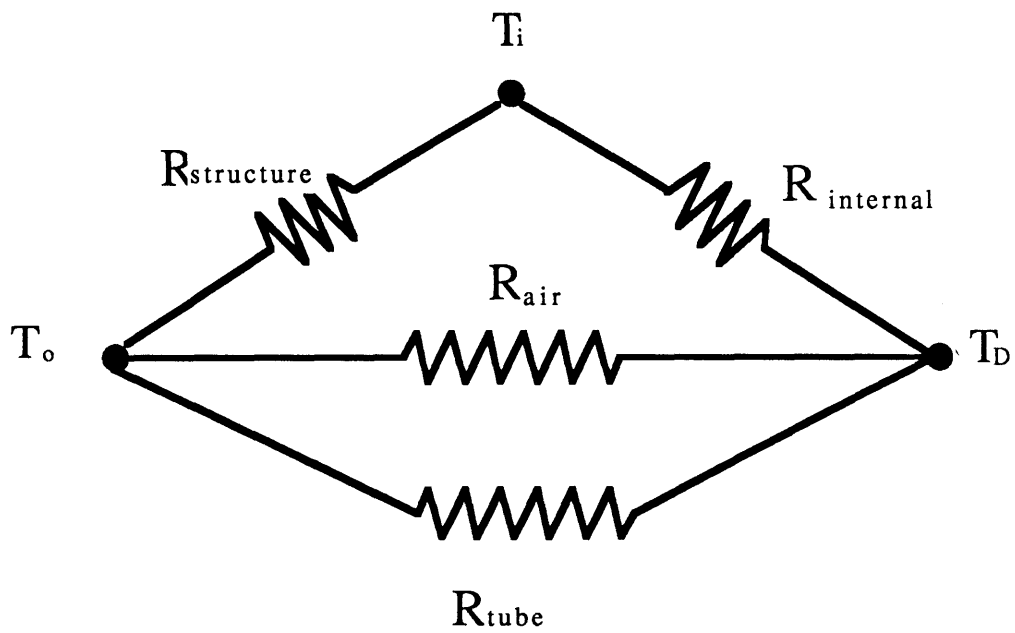


Fig. 8.0.2 1-D Steady State Electrical Equivalent

Convective Heat Transfer: Convective heat transfer can occur inside the pneumatic tube due to temperature difference between boundaries. If convection occurs, the heat flow rate through the air core would be increased. Also, the pressure measurement would be affected due to the existence of internal air flow. The Rayleigh number, which determines the presence of natural convection, is a function of the temperature difference between the boundaries and geometry. The Rayleigh number can be expressed as;¹⁹

$$Ra = \frac{g\beta(\Delta T) r^3}{\nu\alpha}$$

where ΔT = temperature difference
 $\beta = 1/T$
 g = gravitational constant
 ν = kinematic viscosity

If the Rayleigh's number is much less than one, convection can be ignored. Convective heat transfer must be minimized for both thermal considerations and the accuracy of pressure measurements.

Conductive Heat Transfer: If radiative and convective heat transfer is assumed to be negligible, then most of the heat transfer between the vehicle surface and the transducer would be due to conduction. For further simplification of the problem, a one-dimensional, steady-state, electrical equivalent is drawn in Fig. 8.0.2. The heat flows from the node at the vehicle surface temperature T_0 to the node at the transducer diaphragm temperature T_D . The total heat flow between these two nodes determines the thermal load of the transducer. The heat flow routes can be simplified into three different paths. Part of the heat would flow through the pneumatic tube which is placed in between the surface and the transducer. Part of the heat would flow through the air core inside the tube. Also, some portion of the heat flow would transferred through the vehicle skin and heat up the

internal air and structure; and the soaked heat inside the vehicle would raise the transducer temperature. The total heat flow of this sensor system can be described as;

$$q = \frac{T_o - T_D}{\sum R_j}$$

where R_j are the thermal resistances. The air thermal resistance, R_{air} , is just a function of the air temperature and the tube dimension. The thermal resistance of air is very high, therefore the heat flow through the air core is relatively small. The thermal resistance of the vehicle skin structure, $R_{structure}$, is dependent on the vehicle configuration. If thermal insulators and/or active cooling are installed on the vehicle, the heat flow through the structure can be minimized. The thermal resistance of the pneumatic tube, R_{tube} , is a design parameter. This resistance can be increased by selecting materials with low thermal conductivity. Consequently, the transducer thermal requirement is dependent on the vehicle configuration and the orifice materials. By installing thermal insulators and/or active cooling of the sensor system as shown in Fig. 8.0.3, the maximum operating temperature requirement of the pressure transducer can be lowered.

Once the vehicle configuration is determined, a more detailed thermal analysis can be executed by numerical techniques. For the simple pneumatic tube and transducer system, the governing conduction equation can be expressed as;¹⁹

$$\frac{\delta^2 T}{\delta r^2} + \frac{1}{r} \frac{\delta T}{\delta r} + \frac{\delta^2 T}{\delta z^2} = \frac{1}{\alpha} \frac{\delta T}{\delta \tau}$$

and for the steady-state condition;¹⁹

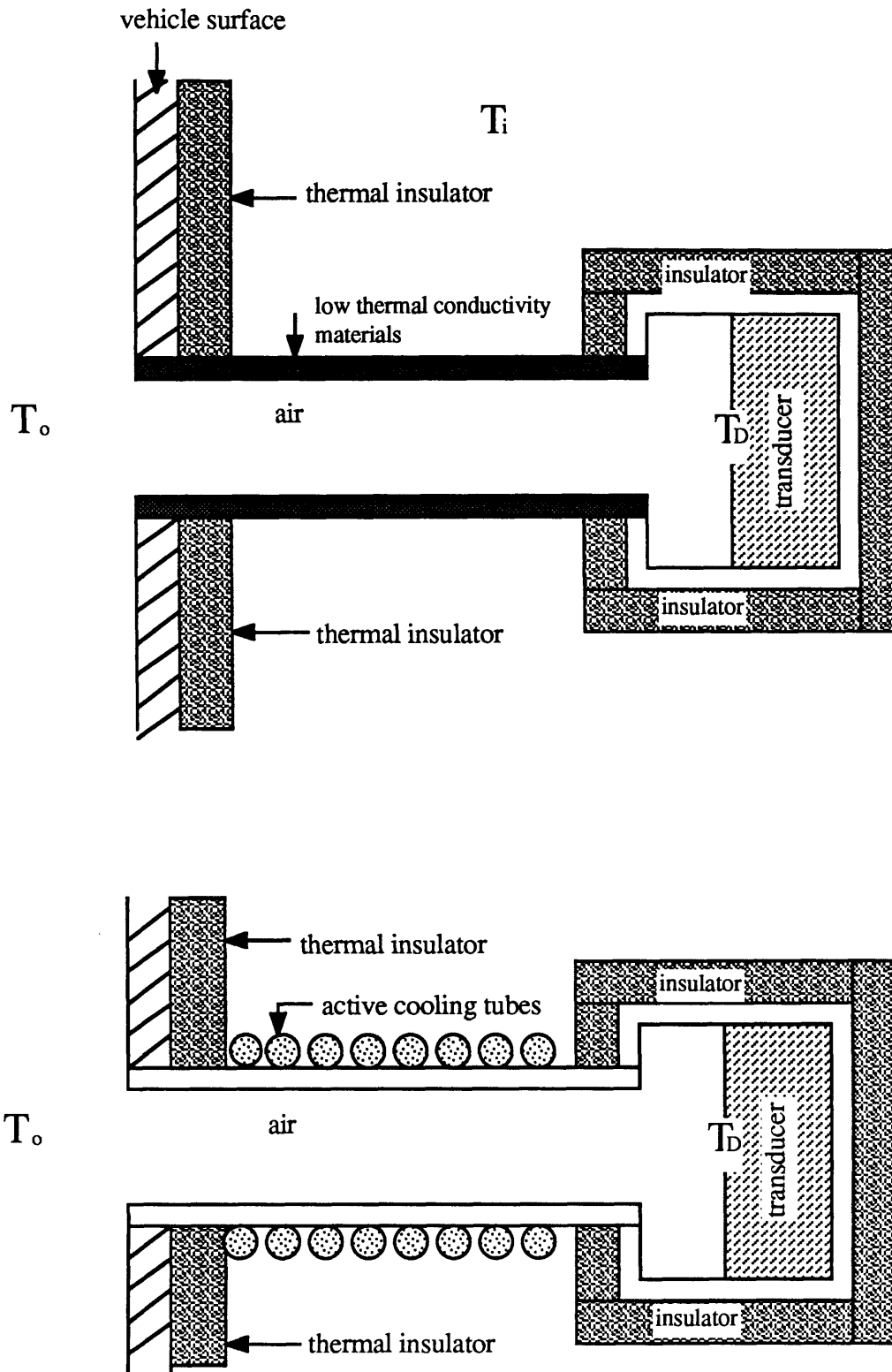


Fig. 8.0.3 Thermal Insulation and Active Cooling

$$\frac{\delta^2 T}{\delta r^2} + \frac{1}{r} \frac{\delta T}{\delta r} + \frac{\delta^2 T}{\delta z^2} = 0$$

with the boundary conditions for the both end of the tube and the tube inner wall;

$T(0,z) = f(z)$	air core temperature axial distribution
$T(R,z) = g(z)$	tube inner wall temperature
$T(r,Z_0) = T_0(r)$	transducer radial temperature distribution
$T(r,0) = T_e(r)$	orifice opening radial temp. distribution

The conductive heat transfer between each end of the pneumatic tube also can be computed in a similar way with different boundary conditions.

8.1 SENSOR INSTALLATION AND DESIGN REQUIREMENTS

The position of the pressure orifices should be in locations where the change in surface pressure are large with respect to the changes in the air data parameters of interest. For example, the flow direction parameters impose the highest surface pressure sensitivity at 45° from the vehicle reference line. For large angle of attack range, the installation of multiple sensors is desirable since the pressure sensitivity decreases as the angle between the normal vector of the surface where the sensor is located and the velocity vector deviates from 45°. An additional installation issue involves alignment. The flush mounted pressure orifice locations on the surface must match with the flow model pressure points. Precision angular alignment with respect to the vehicle reference axis is needed. Angular misalignment will result in flow direction error.

In the implementation of flush orifice pressure sensor techniques, the sensor thermal limitations and sensor geometry should be considered. The vehicle surface and the transducers should be thermally insulated to minimize indirect heat soak. Low thermal conductivity materials should be selected for at least part of the pneumatic tube. Graphite or ceramic are considered for high temperatures insulation, however these materials are extremely brittle. In addition there are installation problems associated with the thermal expansion ratio of the high temperature materials. If the surface structure is constructed with high thermal expansion ratio materials, then the difference in thermal expansion of the orifice and the structure will cause thermal stress problems. Also, bonding between the orifice and the surface structure is extremely difficult due to high temperature at the surface. Therefore it is desirable to construct the orifice and initial pneumatic tube as a part of the surface structure with the same materials.

9.0 PRESSURE TRANSDUCER EVALUATION

9.1 PERFORMANCE REQUIREMENTS

Based on the forebody surface pressure measurement methodology and the hypersonic air data parameter specifications presented in Section 5.4, the pressure transducer performance requirements are presented in Table 5. The transducer requirements are divided into 4 different categories based application.

The transducer specifications for the nose cap sensor array are an operating range of 1000 to 4300psf, a maximum orifice temperature of 3000°F, and an accuracy of 0.3% of max. Based on SEADS like air data sensing technique, the algorithm for angle of attack extraction is inverted to obtain the pressure sensor accuracy requirements based on the angle of attack requirements. In order to resolve a 0.1° angle of attack accuracy, a 0.3% precision pressure transducers are needed. The pressure transducer thermal requirements are dependent on the bandwidth requirements and the orifice design. The bandwidth requirement for the nose cap air data sensor system is estimated to be order of 1Hz. If the angle of attack and angle of attack rate is needed to control the vehicle short period mode for the propulsion system, then the bandwidth requirement would be order of magnitude larger than the short period frequency.

The transducer requirements for the static pressure sensors are a pressure range of 10 to 2100psf, a maximum orifice temperature of 1500°F and an accuracy of 0.3% based on the pressure altitude measurement requirement. The static pressure sensors are normally placed on the side of the fuselage where the surface temperature would be much lower than the stagnation region. Usually high bandwidth measurement is not required.

Pressure Transducer Requirements

<u>Location</u>	<u>Temperature Range</u>	<u>Pressure Range</u>	<u>Accuracy (% Max)</u>
Air Data System			
Nose Cap Area	0 - 3000°F	1000 - 4300psf	0.3%
Static Pressure	0 - 1500°F	10-2100psf	0.3%
Propulsion Control System			
Inlet Array	0 - 3000°F	200 - 4300psf	0.1%
Inlet Differential	0 - 3000°F	200-4300psf	

Table 5

The inlet pressure transducers which detect the inlet flow field will also require high precision and high bandwidth. If such transducers are used inside the inlet control loop, the transducer requirements would have an operating range of 200 psf to 4300 psf, a maximum orifice temperature of 3000°F, and an accuracy of 0.1% of max. In addition, bandwidth requirements of 100Hz to 500Hz may be needed for the inlet controller. Due to the high bandwidth requirements, the inlet pressure transducers would likely be placed near the surface, therefore the transducer itself must endure the 3000°F thermal loads.

The engine yaw detection sensor would utilize differential pressure sensors within the inlet. The transducer requirements would be an operating range of 200 to 4300psf, a maximum orifice temperature of 2000°F.

9.2 APPLICABILITY OF CURRENT TECHNOLOGY SENSORS

Based on the pressure transducer performance requirements of Section 9.1, the applicability of current commercially available pressure transducers was reviewed. The most stringent pressure transducer specification comes from the inlet sensor arrays. Since the transducer must be placed very close to the high temperature surface, the transducer must operate at near 3000 °F while providing 0.1% transducer accuracy. A partial list of representative commercially available pressure transducers is presented in Table 6. Many of the transducers are low pressure high precision piezo-resistive or strain gauge type and a few high temperature, high pressure water cooled strain gauge transducers are also included. The low pressure transducers typically have an operating range of 0 to 2200psf with accuracies between 0.25 and 0.5%. Typical maximum operating temperatures are 250°F and often the transducers are temperature compensated to only 160°F. In general, the accuracy of the transducer decreases with increased operating temperature.

Of those reviewed, there is only one transducer, with a built in active cooling capability, which can meet the 3000°F temperature requirement of the engine inlet sensors. However, this transducer has an accuracy of 1% and cannot meet the accuracy requirements of 0.1% to 0.3%. There are several transducers which can meet the accuracy requirements however their maximum operating temperatures are too low. None of the current pressure transducers which were reviewed could meet both the thermal and accuracy requirements. Therefore, active or passive cooling would be required to employ existing technology high precision transducers.

Current Transducer Performance

Technique	P-Range (psi)	Accuracy (%)	Temp (°F) (max)	Case Volume (in ³)
Strain gauge (uncooled)	0 - 15	0.25 - 1	150 - 600	0.884 - 20.32
Strain gauge (water cooled)	0 - 1000	1	150 - 6000	2.35 - 9.4
Piezoresistive	0 - 20	0.2 - 0.5	150 - 500	0.003 - 0.0909
Silicon on Sapphire	0 - 15	0.1	150 - 250	1.57
Vibrating Quartz Crystal	0 - 20	0.02	230	4.03
Sputtered Thin Film	0 - 15	0.1 - 0.5	300 - 650	1.57 - 1.89
Differential Capacitive	0 - 15	0.08	160	62.9
Hybrid Mechanical	0 - 15	0.021	160	237.5

Table 6

10.0 CONCLUSION

The air data and inlet control measurement requirements for advanced hypersonic vehicles such as the NASP were estimated based on anticipated trajectories and vehicle configurations. Based on the available literature on prior hypersonic air data systems on the X-15, SR-71 and the Shuttle Orbiter, surface pressure based measurement systems such as the Shuttle Entry Air Data System (SEADS) appear to be the most promising candidates for advanced hypersonic vehicles. A SEADS-like forebody pressure distribution system for air data measurement combined with an inlet surface pressure array for active inlet control is considered to be the most viable air data measurement configuration. Due to the stringent requirements on the air data and inlet control parameters, as well as the need to locate the surface pressure sensors in regions of extreme thermal load resulted in rigorous pressure transducer requirements (0.1% accuracy at 3000°F orifice temperature). Existing technology high precision pressure transducers were found to require active or passive cooling in a hypersonic air data system.

REFERENCES

- Ref. 1 Pruet, D, Siemers, P., Heck, M., "An Innovative Air Data System for the Space Shuttle Orbiter: Data Analysis Technique", AIAA Paper 81-2455 1981.
- Ref. 2 Hillje, E., "The Orbiter Air Data System", AIAA Paper 1983.
- Ref. 3 Wolowicz, C. and Gossett, T., "Operational and Performance Characteristics of the X-15 Spherical Hypersonic Flow Direction Sensor", NASA TND-3070, August 1965.
- Ref. 4 Webb, L., "Characteristics and Use of X-15 Air Data Sensors", NASA TN D-4597 Nov. 1967.
- Ref. 5 Larson, T., Webb, L., "Calibration and Comparisons of Pressure-Type Airspeed System of the X-15 Airplane from Subsonic to High Supersonic Speeds", NASA TN D-1724, Dec. 1962.
- Ref. 6 Lehtinen, B., Zeller, J., Geysler, L., "Optimal Control of Supersonic Inlets to Minimize Unstarts", NASA TN D-6408 July 1971.
- Ref. 7 YF-12 Experiments Symposium, Vol.1, NASA Conference Publication 2054, Sept. 1978.
- Ref. 8 Pegg, R.J., "National Aero-space Plane", NASA, Briefing to the Congressional Aeronautical Advisory Committee, March 1988.
- Ref. 9 Personal communication with M. Martinez Sanchez, (MIT Aero & Astro) on March 1988.
- Ref. 10 Shapiro, R., "An Adaptive Finite Element Solution Algorithm for the Euler Equations", Ph.D. Thesis, MIT Dept. of Aero & Astro, May 1988.
- Ref. 11 NASA Conference on Supersonic Missile Propulsion, March, 1952.

- Ref. 12 Goldstein, Richard J., Fluid Mechanics Measurements, Hemisphere Publishing Corporation, 1983, pp. 61 - 97.
- Ref. 13 Lewis, Mark J., "The Prediction of Inlet Flow Stratification and Its Influence on the Performance of Air-Breathing Hypersonic Propulsion System" , Ph.D. Thesis, MIT Dept. of Aero & Astro, June 1988.
- Ref. 14 Personal Communication with P. Gibson , NASA Langley, May 1989
- Ref. 15 Neumann, R.D., "Instrumentation Concepts for 'X'-Series Aircraft", AIAA Paper 88-4650-CP, Sept. 1988.
- Ref. 16 Koppenwallner, G. "Hypersonic Aerothermodynamics", Von Karmann Institute for Fluid Dynamics, Lecture Series 1984-01, Feb. 1984.
- Ref. 17 Cassidy, Michael P., "An Optimization Process For the Scramjet Phase of the Ascent Trajectory of a Next Generation Space Shuttle", S.M. Thesis, MIT Dept. of Aero & Astro, Feb. 1986.
- Ref.18 Sizoo, David G., "The Effects of Dynamic Error Sources on the Altitude Hold Performance of Aircraft Tracking a Pressure Altitude" S.M. Thesis, MIT Dept. of Aero & Astro, Sept. 1986.
- Ref. 19 Holman, J.P., "Heat Transfer", McGraw-Hill Kogakusha LTD., Fourth Edition, 1976.
- Ref. 20 Franklin R.E.,Wallace J.M., "Absolute Measurements of Static-Hole Error Using Flush Transducers", J. Fluid Mech. 1970, vol. 42, part 1, pp. 33-48